UC San Diego

UC San Diego Electronic Theses and Dissertations

Title

The importance of histidine 197 in Escherichia coli release factor 1 and the nucleotide dependence of release factor 3

Permalink

https://escholarship.org/uc/item/4rf6t9bf

Author

Field, Andrew Ryan

Publication Date

2010

Peer reviewed|Thesis/dissertation

eScholarship.org Powered by the California Digital Library
University of California

UNIVERSITY OF CALIFORNIA, SAN DIEGO

The Importance of Histidine 197 in *Escherichia coli* Release Factor 1 and the Nucleotide Dependence of Release Factor 3

A Thesis submitted in partial satisfaction of the requirements for the degree

Master of Science

in

Chemistry

by

Andrew Ryan Field

Committee in charge:

Professor Simpson Joseph, Chair
Professor Ulrich Muller
Professor Navtej Toor
Professor Yitzhak Tor

2010

Copyright

Andrew Ryan Field, 2010

All rights reserved.

The Thesis of Andrew Ryan Field is approved and it is acceptable in quality and form for publication on microfilm and electronically:

_____

_____

_____

_____

Chair

University of California, San Diego
2010

TABLE OF CONTENTS

Signature Page iii

Table of Contents iv

List of Abbreviations viii

List of Figures x

Acknowledgements xi

Vita and Publications xii

Abstract of the Thesis xiii

Chapter 1: Introduction 1

The Role of the Ribosome and Its Structure 1

Ribosome Structure Overview 2

Relevant Structural Features 4

Overview of the Three Phases of Protein Synthesis 5

Initiation and Ribosome Subunit Association 5

Elongation of the Nascent Polypeptide 7

Termination of Translation and Recycling of the Ribosome 7

The Termination Phase of Protein Synthesis and Peptide Release Factors 8

Class I Peptide Release Factors 9

Class II Peptide Release Factors 11

Goal of Thesis 16

RF1 H197A Binding Kinetics 16

Catalysis and Nucleotide Dependence of RF3 17

Chapter 2: Histidine 197 in Release Factor 1 is Essential for A-Site Binding and Peptide Release 18

Introduction 18

Results 20

Equilibrium Binding of H197A RF1 to Ribosome 20

Kinetics of H197A RF1 Binding to Ribosome 22

Kinetics of Peptide Hydrolysis by H197A RF1 28

Discussion 30

Chapter 3: RF3 Nucleotide Dependence 34

Introduction 34

Results 36

RF3 Trap Experiments 36

Equilibrium Binding of RF3 with Excess Guanine Nucleotides..... 39

GTP Hydrolysis 39

Discussion 41

Chapter 4: Materials and Methods..... 45

Buffers, Ribosomes, tRNA, mRNA, and RF1 Preparation 45

Mutant H197A RF1 45

RF3 Purification 46

GDP Purification 46

Fluorescence Measurements and K_D Titrations of RF1 48

Stopped-Flow Binding Kinetics 49

Peptide Release Assay..... 50

RF3 Initial Fluorescence and Trap Experiments 50

Equilibrium Binding of RF3 51

GTP Hydrolysis..... 52

Chapter 5: Summary and Future Goals..... 54

Crystallography Directed Mutagenesis of RF1..... 54

RF3 Mechanistic Studies 55

Pyrene Labeled mRNA Fluorescence Assay 57

References 59

LIST OF ABBREVIATIONS

A (amino acid)	Alanine
A (nucleic acid)	Adenine
Arg	Arginine
A-Site	Aminoacyl Site
C	Cytosine
DNA	Deoxyribose Nucleic Acid
EF	Elongation Factor
E-Site	Exit Site
G	Guanine
GAC	GTPase Activation Center
GDP	Guanosine Diphosphate
GDPNP	5'-Guanylyl Imidodiphosphate
Gln	Glutamine
Glu	Glutamic Acid
Gly	Glycine
GTP	Guanosine Triphosphate
H	Histidine
His	Histidine
His-Tag(ged)	C-Terminal 6-Histidine Tag(ged)
HPLC	High-Performance Liquid Chromatography
IF	Initiation Factor

kDa	Kilodalton
mRNA	Messenger Ribonucleic Acid
P-Site	Peptidyl Site
Pro	Proline
PTC	Peptidyl Transferase Center
RC	Release Complex
RF1	Release Factor 1
RF2	Release Factor 2
RF3	Release Factor 3
RNA	Ribonucleic Acid
rRNA	Ribosomal Ribonucleic Acid
T	Thymine
Thr	Threonine
tRNA	Transfer Ribonucleic Acid
U	Uracil
Val	Valine

LIST OF FIGURES

Figure 1.1: Ribosome structure with RF1 structural features 3

Figure 1.2: Protein synthesis overview 6

Figure 1.3: Release factor extension 10

Figure 1.4: Key residues in RF1 stop-codon recognition 12

Figure 1.5: Ehrenberg RF3 mechanism 14

Figure 1.6: RF3-GDP structure 15

Figure 2.1: Structure of RF1 bound to the ribosome 21

Figure 2.2: Fluorescence assay for determining the K_D of H197A RF1 22

Figure 2.3: Kinetics of H197A binding to the ribosome 25

Figure 2.4: Peptide release time course and a schematic model for RF1 binding and peptide release 29

Figure 3.1: Initial RF3 fluorescence time scans 37

Figure 3.2: RF3 trap experiments 38

Figure 3.3: RF1 K_D with RF3 and nucleotides 40

Figure 3.4: RF3 GTP hydrolysis 42

Figure 4.1: RF3 SDS-PAGE gel 47

Figure 4.2: Dionex DNA Pac PA-100 HPLC GDP purification 48

Figure 4.3: RF3 “equilibrium” 52

ACKNOWLEDGEMENTS

I would like to thank Professor Simpson Joseph for accepting me into his lab, his guidance through my project and his support as my principle investigator and thesis committee chair. Byron Hetrick was a great asset for guidance, knowledge and help with techniques as well as concepts in the lab. Merrill Mathew was a hard working undergraduate student of great assistance in lab who toiled tirelessly to produce essential data for my research. In addition, I would like to thank Prashant Khade, Xingying Shi and Eileen Chen for their kind and thoughtful help especially when I was new to the lab. This work would not be possible without any of these people.

The UCSD Biochemistry department office has been a great asset as well. Jeff Rances in particular has shown nothing but kindness and extreme helpfulness through all aspects of my graduate career. Without his help, I would still be lost in paperwork.

The support of my family has been unwavering throughout my educational career. My mother and father, Deborah and Steven Field, have never declined to help in any way they could whether it be financial or epicurean.

Portions of chapter 2 and 4 are reproduced in part with permission from Field, A.; Hetrick, B.; Mathew, M.; and Joseph, S. (2010) Histidine 197 in release factor 1 is essential for A-site binding and peptide release, pending publication in *Biochemistry*, submitted July 29, 2010.

VITA

2001-2004 Los Angeles Pierce College

2004-2008 Bachelor of Science in Biochemistry, Rochester Institute of Technology

2008-2010 Master of Science in Chemistry, University of California, San Diego

Publications

Field, A., B. Hetrick, M. Mathew and S. Joseph (2010). “Histidine 197 in release factor 1 is essential for A-site binding and peptide release”. Pending publication in *Biochemistry*. Submitted July 29, 2010.

ABSTRACT OF THE THESIS

The Importance of Histidine 197 in *Escherichia coli* Release Factor 1 and the Nucleotide Dependence of Release Factor 3

by

Andrew Ryan Field

Master of Science in Chemistry

University of California, San Diego, 2010

Professor Simpson Joseph, Chair

Class I peptide release factors 1 and 2 (RF1 and RF2) are responsible for accurate termination of protein synthesis by high fidelity recognition of stop codons in the decoding center of the ribosome. Analyses of crystal structures have revealed specific residues at the mRNA – release factor interface

that appear crucial for decoding center binding (Laurberg, et al. 2008; Wiexlbaumer, et al. 2008; Korostelev, et al. 2008). Due to intricate associations of class I release factors to the A-site, an addition class II release factor, RF3, is required for their removal (Freistroffer, Pavlov, et al. 1997).

A recently developed fluorescence based method to monitor decoding center interactions (Hetrick, Lee and Joseph 2009) was utilized to investigate the importance of histidine 197 (H197) in RF1 binding. The change in fluorescence of a pyrene probe attached to mRNA accurately determined the presence of RF1 in the A-site. H197 was found to be crucial for both efficient binding to the mRNA and orientation of the RF for catalysis of peptide release. RF1 was also found to bind in a biphasic manner. An adapted version of the assay was used to study the functional requirements of RF3 mediated removal of RF1. This proved useful in detecting RF1 release from the decoding center with RF3 and GTP, but the protein seemed to lack GTPase activity over basal ribosomal levels. In addition, no release was observed with GDPNP which was contrary to previous studies (Zavialov, Buckingham and Ehrenberg 2001; Zavialov, Mora, et al. 2002).

Chapter 1: Introduction

The role of the ribosome and its structure

The central dogma of molecular biology states that information in the cell is passed from DNA to RNA to protein (Crick 1970). A key step in this process is the translation of messenger RNA (mRNA) to protein facilitated by the ribosome and aminoacyl-transfer RNAs (tRNA). All known life utilizes the ribosome for this action and without accurate protein synthesis life as it exists today could not function.

In addition to tRNA, there are also numerous protein factors involved in regulating this process. During the initiation phase of translation, initiation factors (IFs) coordinate recruitment of mRNA and the association of ribosomal subunits. Elongation factors (EFs) ensure the proper loading and translocation of the ribosome complex. Finally, release factors (RFs) ensure accurate termination of protein synthesis and begin the recycling of the ribosomal subunits. Recent crystal structures have made it possible to look more in depth into individual protein residues and their contribution to these mechanisms (Schmeing and Ramakrishnan 2009). The focus of this thesis will be on the importance of a histidine residue in the stop codon interaction region of class I release factor RF1 and the kinetics of class II release factor RF3 catalysis.

Ribosome structure overview

The prokaryotic ribosome is a 2.6-megadalton ribonucleoprotein complex composed of approximately two-thirds ribosomal RNA (rRNA) and one-third protein (Kurland 1960). The complete 70S complex can be broken into two major subunits: the 30S small subunit and 50S large subunit (Kurland 1960). One 16S rRNA fragment and about 20 proteins make up the small subunit where 23S and 5S rRNA with about 30 proteins compose the large subunit (Kurland 1972). In eukaryotes, the 70S ribosome is replaced with the 80S ribosome which is composed similarly of two subunits denoted as the 40S and 60S respectively (Schmeing and Ramakrishnan 2009).

High resolution crystal structures of the separate prokaryotic 30S and 50S subunits opened the gateway to the first structural insights into the inner-workings of the ribosome (Ban, et al. 2000; Wimberly, et al. 2000). Following these studies, the structure of the complete 70S ribosome with tRNAs bound was solved at low resolution providing further structural information of the ribosome in a functional state (Yusupov, et al. 2001). Many more structures have since been solved revealing molecular details of intermediate functional states (Figure 1.1) (Schmeing and Ramakrishnan 2009).

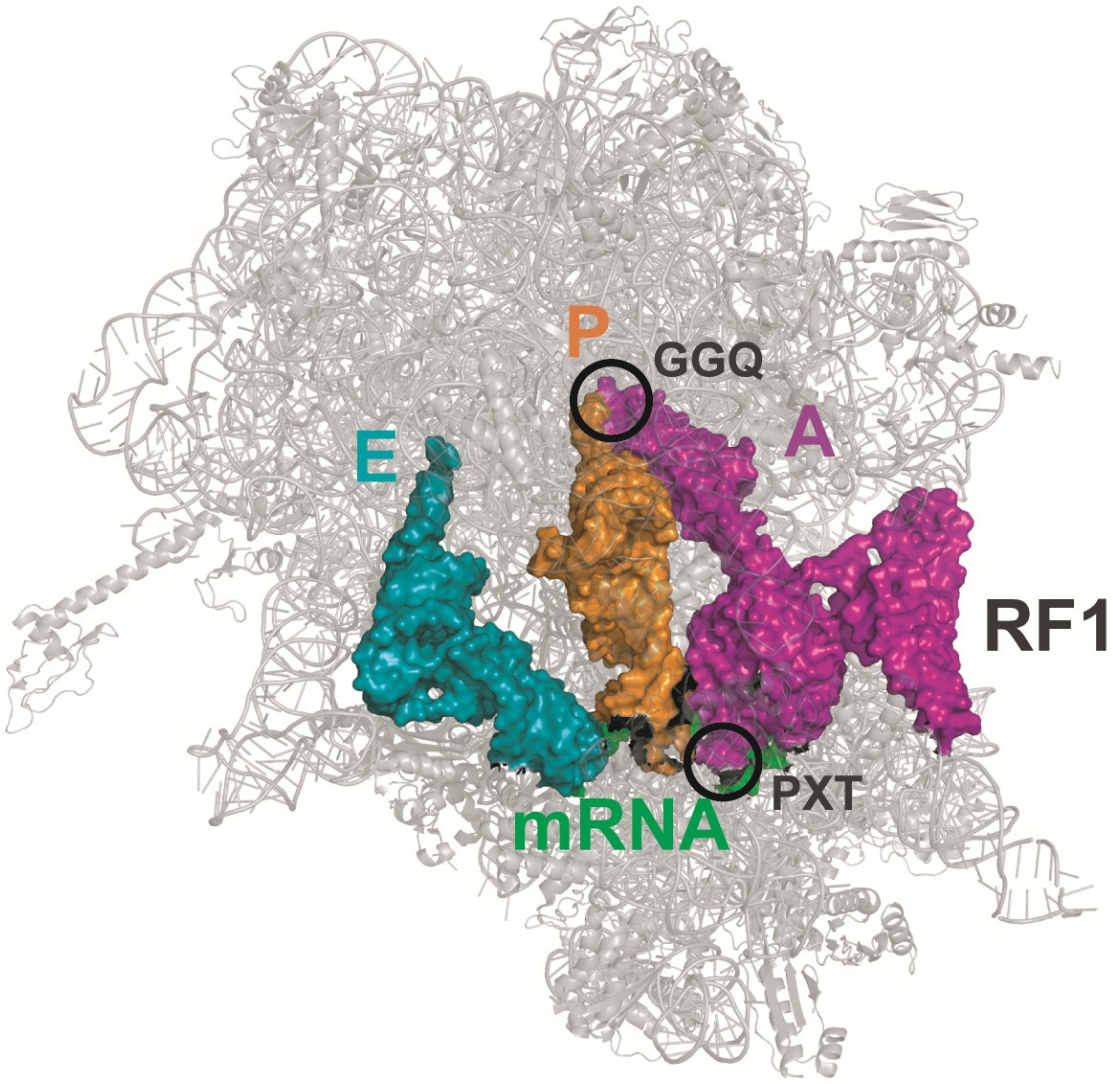

Figure 1.1: Ribosome structure with RF1 structural features. Above is the structure of the 70S ribosome termination complex from *Thermus thermophilus* with a UAA stop codon and bound RF1 at 3.2 Å resolution. 70S ribosome with associated proteins (gray), mRNA (green), RF1 in the A-site (purple), P-site tRNA (orange), and E-site tRNA (teal). The PXT domain in the decoding center and GGQ in the PTC are also indicated. The structure was prepared using PyMol. Protein Data Bank ID 3D5A and 3D5B (Laurberg, et al. 2008).

Relevant structural features

The mRNA binds in a cleft located on the 30S subunit (Yusupova, et al. 2006). tRNA interacts directly with the mRNA on this cleft in three sites at the interface of the 50S and 30S subunits. These sites are labeled the A, P, and E-sites (Figure 1.1) (Moazed and Noller 1989). The A-site, or aminoacyl site, is where new aminoacyl-tRNAs are accepted onto the ribosome and selected by direct base pair interactions with the mRNA (Yusupov, et al. 2001; Wimberly, et al. 2000). Directly adjacent to the A-site on the mRNA is the peptidyl site, or P-site, which holds the peptidyl-tRNA (Yusupov, et al. 2001). Before being ejected from the ribosome, deacylated tRNA is transferred to the E-site (exit site) adjacent to the P-site on the mRNA but located some distance away on the 50S subunit (Yusupov, et al. 2001).

In addition to the three tRNA sites on the ribosome, there are several other important catalytic domains. The peptidyl transferase center (PTC) is located between the A and P sites on the 50S subunit (Figure 1.1). This is where the peptide attached to the peptidyl-tRNA in the P-site is transferred to the new aminoacyl-tRNA in the A-site prior to translocation (Traut and Monro 1964). Cryo-electron microscopy (CryoEM) studies have also located two regions important for the GTPase activity of RF3 as well as other GTPase protein factors: the sarcine ricin loop (SRL) and GTPase activation center (GAC) (Klaholz, Myasnikov and Van Heel 2004).

Overview of the three phases of protein synthesis

The process of ribosomal protein synthesis can be described in three main phases: initiation, elongation and termination (Figure 1.2) (Lucas-Lenard, Protein biosynthesis 1971). During initiation, the ribosomal subunits are assembled around the mRNA. The 70S ribosome then transitions into elongation where protein is assembled with the assistance of tRNAs reading the mRNA sequence. Finally, the ribosome is terminated when it reaches a stop codon on the mRNA. At this point, the nascent polypeptide is released and the ribosome complex is disassembled for recycling.

Initiation and ribosome subunit association

In prokaryotes, the ribosome begins as two separate subunits, the 30S and 50S, at the beginning of initiation (Subramanian, Ron and Davis 1968). mRNA is aligned on the 30S subunit, an initiator tRNA is placed in the P-site on the 30S subunit and the 50S subunit is associated with the assistance of initiation factors IF1, IF2, and IF3 (Myasnikov, et al. 2009; Gold, et al. 1981; Nomura and Lowry 1967; Guthrie and Normura 1968). This leaves the A-site open and ready to accept a new aminoacyl-tRNA to begin the elongation cycle.

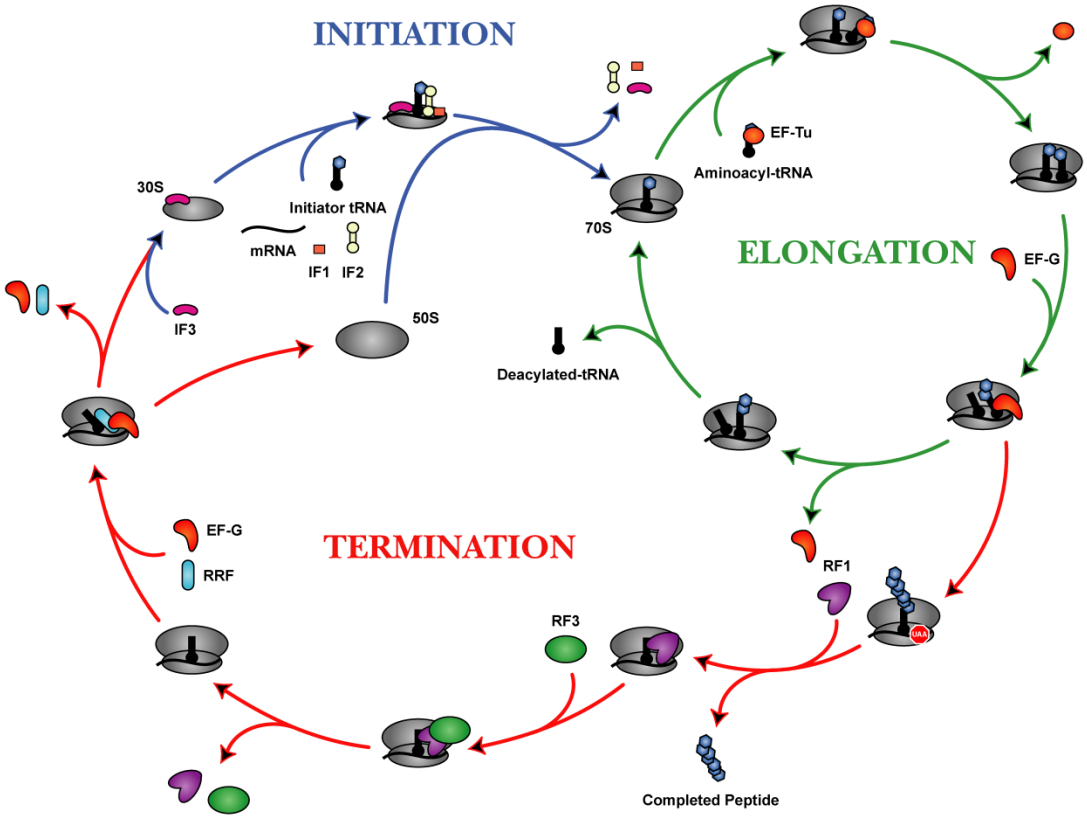

Figure 1.2: Protein synthesis overview. During initiation (blue arrows), the ribosomal subunits are assembled around an mRNA and initiator tRNA assisted by initiation factors IF1, IF2, and IF3. Immediately following, elongation (green arrows) occurs as new aminoacyl-tRNAs are recruited to the ribosome escorted by EF-Tu. Upon hydrolyzing GTP, EF-Tu releases the tRNA into the A-site. The ribosome then catalyzes the transfer of the peptide from the P-site tRNA to the A-site tRNA via peptide bond formation in the PTC. The tRNAs are then translocated from the A-site to P-site and P-site to E-site respectively by EF-G with GTP hydrolysis. Now with a vacant A-site, the elongation cycle continues until a stop codon is reached beginning termination (red arrows). During termination, a class I release factor (shown here as RF1) binds to the A-site catalyzing peptide release. RF3 releases the class I release factor in a GTP dependent manner. Immediately following this, the ribosomal subunits, P-site tRNA, and mRNA are disassembled with RRF and EF-G upon GTP hydrolysis. IF3 then binds to the 30S subunit to prevent premature reassociation and the cycle can continue by repeating initiation.

Elongation of the nascent polypeptide

Aminoacyl-tRNAs are recruited by EF-Tu and inserted into the empty A-site (Lucas-Lenard and Lipmann 1966). A correct tRNA is selected by direct base pair interaction with the tri-nucleotide mRNA sequence aligned in the A-site known as a codon (Rodnina, Fricke and Wintermeyer 1994). This tRNA is then released into the A-site upon EF-Tu mediated GTP hydrolysis (Lucas-Lenard and Lipmann 1966; Swart and Parmeggiani 1989). After A-site insertion, the ribosome catalyzes the transfer of the P-site tRNA bound polypeptide to the A-site bound aminoacyl-tRNA in the PTC (Traut and Monro 1964). EF-G catalyzes a three nucleotide shift in mRNA with respect to the ribosome known as translocation (Lucas-Lenard and Lipmann 1966; Bretscher 1968). This process effectively shifts the tRNA from A-site to P-site and P-site to E-site respectively (Skogerson and Moldave 1968; Rheinberger, Sternbach and Nierhaus 1981). Now, with an empty A-site containing a new codon exposed on the mRNA, the ribosome is able to accept a new aminoacyl-tRNA thus repeating the cycle (Joseph and Noller 1998; Kurland 1972).

Termination of translation and recycling of the ribosome

The codons UAA, UAG and UGA are called nonsense or stop codons because they do not code for tRNA and signal for the end of translation (Brenner, Stretton and Kaplan 1965; Zipser 1967; Petry, Weixlbaumer and Ramakrishnan

2008). When one of these codons enters the A-site, they are recognized by a class I release factor protein initiating the termination phase (Scolnick, et al. 1968; Petry, Weixlbaumer and Ramakrishnan 2008). In prokaryotes, there are two class I release factors known as release factor 1 (RF1) and release factor 2 (RF2) (Scolnick, et al. 1968). These release factors differ in their specificity for stop codons. RF1 recognizes UAA and UAG where RF2 recognizes UAA and UGA (Scolnick, et al. 1968). The primary function of these class I release factors is to catalyze the release of the nascent polypeptide from the peptidyl-tRNA in the P-site (Brown and Tate 1994). Next, the class I release factor is removed by the class II release factor, release factor 3 (RF3), in a GTP dependent manner (Freistroffer, Pavlov, et al. 1997). This then allows for ribosome recycling factor (RRF) and EF-G to catalyze the disassembly of the ribosomal complex into its respective subunits (Karimi, et al. 1999). IF3 binds the freed 30S to prevent premature re-association of the subunits (Subramanian, Ron and Davis 1968). With the subunits separated, the ribosome is free to begin the initiation cycle again.

The termination phase of protein synthesis and peptide release factors

Although the functions of class I and class II release factors are well known, the details of the structures, mechanisms and kinetics are just recently beginning to elucidate. The residues necessary for accurate termination by class

l release factors and the mechanism of their removal by RF3 are still under scrutiny.

Class I peptide release factors

Stop codon recognition by class I release factors occurs without the aid of a proofreading mechanism yet is surprisingly more accurate than tRNA decoding (Petry, Weixlbaumer and Ramakrishnan 2008). RF1 and RF2 also allow for the flexibility of a G or an A in the third and second codon positions respectively. This suggests a complex recognition event with incredibly high fidelity and specificity that is not seen in the decoding of sense codons.

Initial experiments to identify the important residues of stop codon recognition uncovered a "tripeptide anticodon" motif of P(A/V)T (also PXT) in RF1 and SPF in RF2 (Figure 1.1, Figure 1.3 and Figure 1.4) (Ito, Uno and Nakamura 2000). As the name suggests, the authors hypothesized that the tripeptide motif acted in a similar manner to the tRNA anticodon by directly matching amino acid to nucleotide in the decoding center.

Mutational experiments also suggested that a universally conserved GGQ motif found in both prokaryotic and eukaryotic release factors is necessary for peptide release (Figure 1.1 and Figure 1.3) (Frolova, et al. 1999). In unbound crystal structures, the GGQ motif is disordered and the RF is found in a compact conformation (Vestergaard, et al. 2001). When bound to the ribosome however, the GGQ motif is highly structured and extended into the PTC possibly

suggesting a conformational change of the release factor upon binding (Figure 1.3) (Petry, Brodersen, et al. 2005).

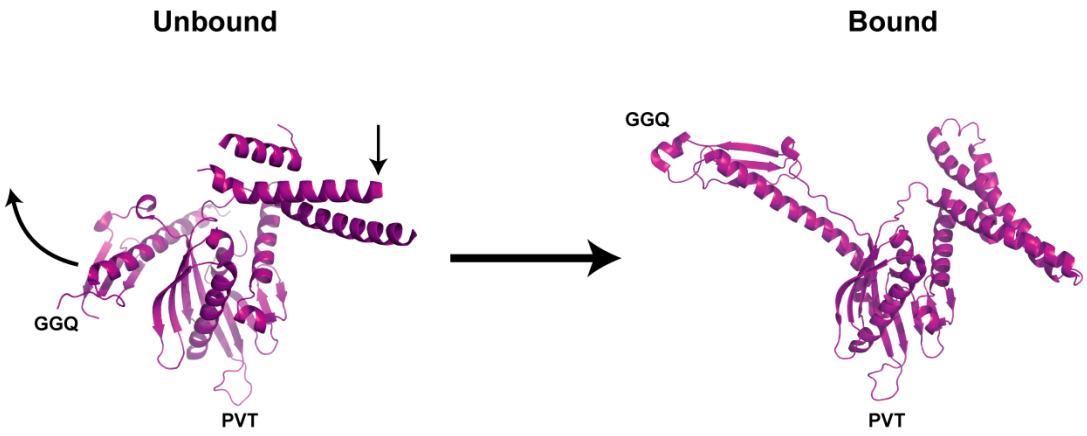

Figure 1.3: Release factor extension. The above shows the two observed conformations of RF1 in crystal structures. The left structure shows the unbound RF1 from *Streptococcus mutans* in a tight conformation where the right is the structurally homologous *Thermus thermophilus* RF1 bound to the A-site of the ribosome with a structured GGQ motif extended into the PTC. The arrows on the unbound structure indicate the possible motion of the respective RF1 domains when it binds to the ribosome. The structure figures were prepared using PyMol. Protein Data Bank ID 1ZBT and 3D5A (Laurberg, et al. 2008).

X-ray crystallography at high resolution has produced a multitude of residues within close contact to the bases of the stop codon (Figure 1.4) (Laurberg, et al. 2008; Wiexlbaumer, et al. 2008; Korostelev, et al. 2008). These studies show both “tripeptide anticodons” interacting only with the first and second nucleotide positions and identify an additional “anticodon” loop (Figure 1.4A) (Petry, Brodersen, et al. 2005). In RF1, the first position U (U1 in Figure 1.4A) also interacts with the backbone of Gly116 and Glu119 as well as the side chain of Thr186 (*Thermus thermophilus* numbering). The second position A (A2

in Figure 1.4B) stacks against the side chains of Glu119 and Pro184 while Thr186 interacts directly with the base. In the third position (A3 in Figure 1.4C), Gln181 and Thr194 work in tandem to recognize either a G or an A (Sund, Ander and Aqvist 2010). Interestingly, in both RF1 and RF2, there is a conserved histidine (H193 in *Thermus thermophilus,* or H197 in *E.coli,* RF1) that is inserted between the second and third base of the stop codon (Laurberg, et al. 2008; Wiexlbaumer, et al. 2008). This histidine stacks against the base at the second position and promotes the stacking interaction of the third position base with G530 of the 16S rRNA. This also serves to distort the mRNA backbone causing A1492 of the 16S rRNA to move out from helix 44. A1913 of 23S rRNA is then free to stack with A1493 of 16S rRNA which enable tighter binding of the RF (Figure 1.4D).

Class II peptide release factors

The function of prokaryotic RF3 is to promote dissociation of class I release factors from the termination complex following peptide release (Freistroffer, et al. 1997; Zavialov, Buckingham and Ehrenberg 2001). It has been known that RF3 completes this task in a GTP dependent manner (Grentzmann, et al. 1998), but an exact mechanism has been difficult to obtain. RF3 has been shown to both stimulate and inhibit release of P-site bound fMet-tRNA^{fMet} in the presence of GTP, when according to its function, it should stimulate the turnover of class I release factors and increase the extent of

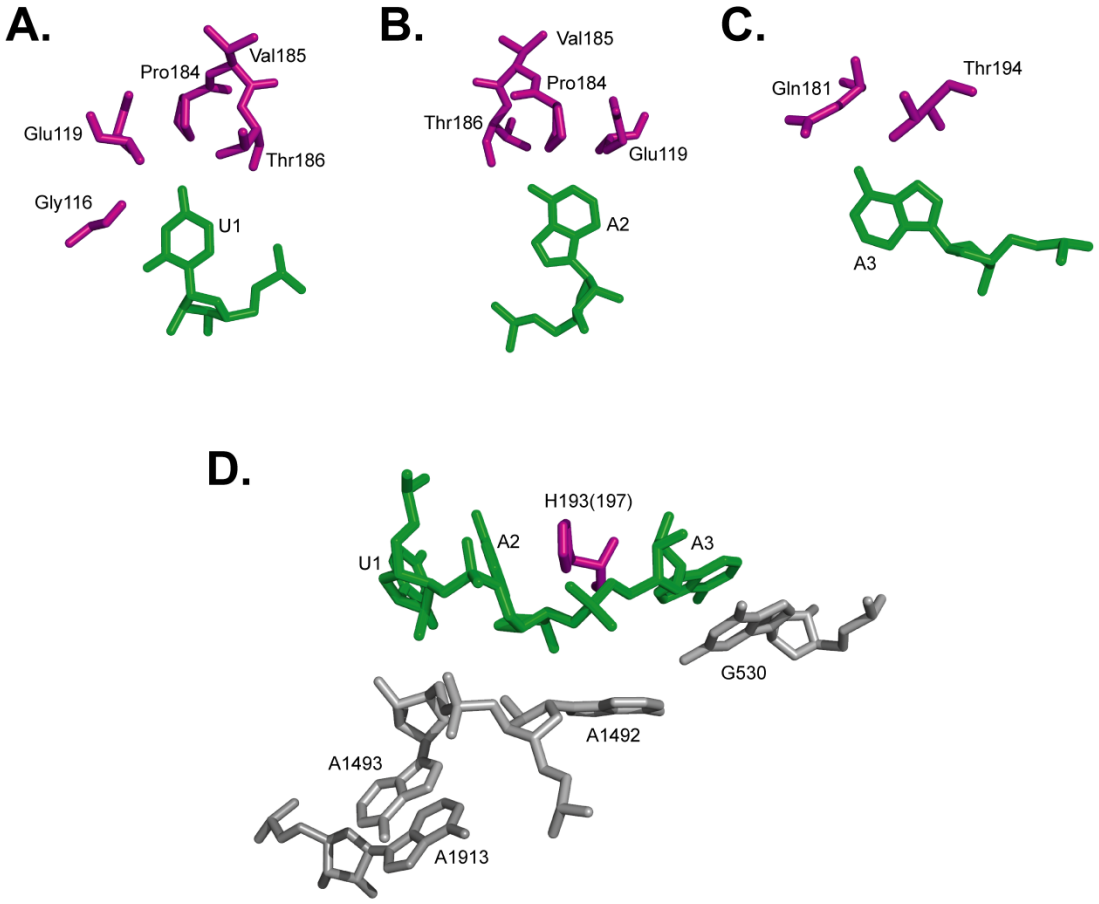

Figure 1.4: Key residues in RF1 stop-codon recognition. RF1 residues (purple), mRNA (green), and rRNA (gray). Crystal structure was obtained from *Thermus thermophilus* RF1 bound to UAA on the ribosome. (A) The first codon position (U1) interacts with Gly116, Glu119, and Thr186 of RF1. (B) The Pro184 and Thr186 from the PXT motif hydrogen-bond to the second position A (A2) along with Glu119. (C) Gln181 and Thr194 stabilize the third position A (A3) as described. (D) H193 (H197 in *E. coli*) is shown unstacking A2 and A3. This allows for stacking of G530 of 16S rRNA to A3 which in turn distorts the backbone of the mRNA and rearranges A1492 of 16S rRNA. The stacking interaction of 16S rRNA A1493 and 23S rRNA A1913 further stabilizes the binding complex. The structure figures were prepared using PyMol. Protein Data Bank ID 3D5A and 3D5B (Laurberg, et al. 2008).

release (Goldstein and Caskey 1970; Mortensen, et al. 1995). These results were not only contradictory but also highly dependent on buffer conditions (Zavialov, Buckingham and Ehrenberg 2001).

More recent experiments have utilized a tetrapeptide release assay with limiting amounts of the class I release factor RF2 compared to the release complex (RC) concentration (Zavialov, Buckingham and Ehrenberg 2001; Zavialov, Mora, et al. 2002). RC consisted of 70S ribosomes prepared with peptidyl-tRNA in the P-site attached to the labeled tetrapeptide and a stop codon in the A-site. These ribosomes were then treated with limiting amounts of RF2 and the rate of peptide release was observed after the addition of RF3 with and without nucleotides. The rate of observed peptide release was used to approximate the rate of RF2 release from the termination complex as significant recycling of the class I release factor was required for complete hydrolysis of the labeled peptides (Zavialov, Buckingham and Ehrenberg 2001). These experiments suggested that RF3 is found in its GDP form off the ribosome, recycling of RF2 requires the exchange of GDP for GTP while RF3 is bound to the ribosome, and recycling of RF3 requires GTP hydrolysis (Zavialov, Buckingham and Ehrenberg 2001). It has also been shown that RF3 binds tightly to the ribosome with a non-cleavable GTP analog (GDPNP) without class I release factors present (Pel, et al. 1998) and optimal rates of GTP hydrolysis can be achieved with just RF3 and ribosomes (Freistroffer, et al. 1997; Grentzmann, et al. 1998). Further studies utilizing GGQ mutants of class I release factors

revealed that peptide release is necessary prior to nucleotide exchange on the ribosome (Zavialov, Mora, et al. 2002).

Upon compiling the data, a mechanism was proposed which addressed some of the apparent inconsistencies (Figure 1.5) (Zavialov, Buckingham and Ehrenberg 2001; Zavialov, Mora, et al. 2002). RF3 with bound GDP joins the ribosome after class I release factor mediated peptide release. The GDP is then exchanged on the ribosome for GTP causing a conformational change in RF3 and catalyzing the release of the class I release factor from the A-site. GTP hydrolysis then returns RF3 to its original conformation allowing for dissociation of the class II release factor. The ribosome, now devoid of all release factors, then moves on for dissociation and recycling by RRF and EF-G.

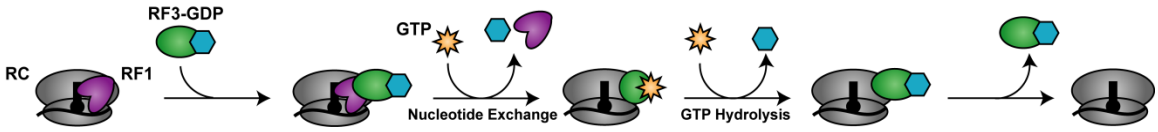

Figure 1.5: Ehrenberg RF3 mechanism. RF3 binds to the RC in the GDP-bound form. Provided that the nascent polypeptide had been released from the P-site tRNA, GDP is exchanged on the ribosome for GTP. A conformational change in the RF3 upon GTP binding loosens the class I release factor (labeled RF1 here) and allows for its dissociation. GTP hydrolysis by RF3 is then required for its own release from the RC (Zavialov, Buckingham and Ehrenberg 2001; Zavialov, Mora, et al. 2002).

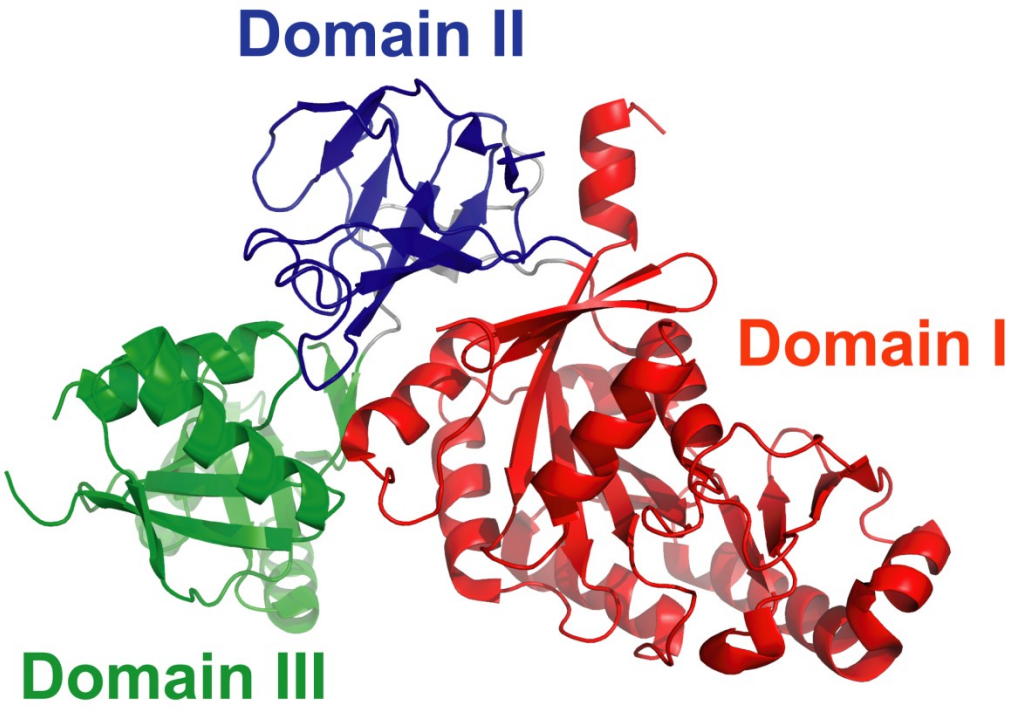

Figure 1.6: RF3-GDP structure. The X-ray crystal structure of RF3 bound to GDP is shown above split into three domains. Domain I is the location of the GTPase activity and is also referred to as the G-domain. Domain II is homologous to domains found on EF-Tu and EF-G and may serve a role in ribosome binding or protein function. Domain III shows no known homology to other ribosomal proteins and its function is unknown. Currently, no high resolution structures are available for RF3 in a ribosome bound state. The structure was prepared using PyMol. Protein Data Bank ID 2H5E (Gao, et al. 2007).

Cryo-EM and crystallography studies have also been conducted on bacterial RF3. RF3-GDPNP bound to ribosomes with P-site tRNA has yielded two low-resolution but still distinct states in cryo-EM (Klaholz, Myasnikov and Van Heel 2004). State one shows a largely unaltered ribosome with the tRNA still intact in the P-site. State two, however, shows a large scale conformational change in which the tRNA is “pushed” into the E-site and the A-site is distorted in the decoding center such that it can no longer accommodate a class I release

factor, perhaps providing a structural basis for release factor ejection. An x-ray crystal structure of RF3-GDP (Figure 1.6) was fit to these cryo-EM structures. No overlap in the class I and class II release factor binding sites was observed but a positional and conformational change in the RF3 was revealed that oriented the G-domain into the GAC (Gao, et al. 2007). The ribosomal subunits also undergo a rotation event similar to EF-G mediated translocation except it does not result in a shift of RF1 or RF2 to the P-site (Agrawal, et al. 1999; Stark, et al. 2000; Klaholz, Myasnikove and Van Heel 2004; Gao, et al. 2007).

Goal of Thesis

RF1 H197A binding kinetics

Recent crystal structures of RF1 bound to the ribosome have revealed a multitude of previously uninvestigated residues that seem important for stop-codon recognition (Petry, Brodersen, et al. 2005; Laurberg, et al. 2008; Petry, Weixlbaumer and Ramakrishnan 2008). Among these is histidine 197 (in *E.coli* numbering) which is highly conserved among bacterial class I release factors. The histidine inserts itself between the second and third position of the stop codon and promotes the stacking of the third position nucleotide with G530 of the 16S rRNA. This leads to stabilization of the mRNA backbone against A1492 of the 16S rRNA (Laurberg, et al. 2008). Here we will investigate the importance of this residue via fluorescence-based transient-state kinetic analysis (Hetrick, Lee

and Joseph 2009) of the mutant H197A. The catalytic functionality of this mutant will also be tested by the rate of peptide release. These studies set the groundwork for future experimentation of the other residues important for the process of class I release factor decoding.

Catalysis and nucleotide dependence of RF3

Although a detailed mechanism of RF3 function has been proposed (Zavialov, Buckingham and Ehrenberg 2001; Zavialov, Mora, et al. 2002), an assay directly measuring its catalysis of class I RF release has yet to be performed. The catalysis of RF1 or RF2 removal from the ribosome has thus far been approximated by the peptide release of recycled release factors. We aim to create an assay that directly observes the release of A-site bound RF1 upon stimulation with RF3 and guanine nucleotides. Utilizing a recently described fluorescence based assay for decoding center binding using pyrene labeled mRNA (Hetrick, Lee and Joseph 2009), we can directly detect the release of RF1 and determine the nucleotide dependence of RF3 catalysis.

Chapter 2: Histidine 197 in Release Factor 1 is Essential for A-Site Binding and Peptide Release

Introduction

The entry of a stop codon into the ribosomal A site signals the termination phase of protein synthesis. The nearly universally conserved stop codons UAA, UAG, and UGA are recognized by class I release factors (RFs) (Brenner, Stretton and Kaplan 1965). In bacteria, there are two class I release factors: RF1 and RF2. RF1 recognizes UAA and UAG, while RF2 recognizes UAA and UGA (Scolnick, et al. 1968). In eukaryotes, a single class I release factor, eRF1, recognizes all three stop codons (Konecki, et al. 1977). Following the recognition of the stop codon in the A site, class I release factors trigger peptidyl-tRNA hydrolysis and the release of the newly synthesized protein from the ribosome (Capecchi 1967). Accurate recognition of stop codons by RFs is essential to prevent premature termination, which would be costly to the cell. The fidelity of stop codon recognition by RFs has been estimated to be 1×10^{-3} to 1×10^{-6} (Jorgensen, et al. 1993; Freistroffer, Kwiatkowski, et al. 2000), which is arguably more accurate than tRNA selection on cognate codons. Remarkably, this high level of accuracy in stop codon recognition is achieved by RFs without the help of a proofreading mechanism.

Previously, the kinetics of RF1 and RF2 discrimination between stop and sense codons were systematically analyzed under steady state conditions

(Freistroffer, Kwiatkowski, et al. 2000). These studies showed that a sense codon in the decoding center increases the K_M between the release factors and the ribosome by 400–3000-fold, while the catalytic rate constant for peptide release (k_{cat}) was reduced by 2–180-fold (Freistroffer, Kwiatkowski, et al. 2000). Thus, discrimination seems to be achieved by the RFs mainly at the binding step. However, binding was not measured directly (K_M is not equal to K_D) and changes in k_{cat} may also occur with improper placement of the RFs in the ribosome.

More recently, the binding of RF1 to ribosomes with stop or sense codons in the decoding center was directly measured using a fluorescence-based, pre-steady state kinetic assay (Hetrick, Lee and Joseph 2009). These studies showed that the association rate constant of RF1 with the ribosome is similar with both sense and stop codons, while the dissociation rate constant increased by as much as 4000-fold when a sense codon is present in the decoding center. Furthermore, defects in RF1 binding to the ribosome do not always correlate with a reduced rate of peptide release suggesting that conformational changes in the ribosome•RF complex occur prior to catalysis (Hetrick, Lee and Joseph 2009).

A conserved “anticodon tripeptide” motif (PXT in RF1 and SPF in RF2) that is important for the specificity of stop codon recognition was identified by genetic analysis (Ito, Uno and Nakamura 2000). More recent X-ray crystal structures of RF1 or RF2 bound to the ribosome have shown additional residues that may also be used for stop codon recognition (Laurberg, et al. 2008; Wiexlbaumer, et al. 2008; Korostelev, et al. 2008). Strikingly, in both RF1 and RF2, the imidazole ring of a conserved histidine (residues 193 and 203 of

Thermus thermophilus RF1 and RF2, respectively) is inserted between the second and the third base of the stop codon (Wiexlbaumer, et al. 2008; Korostelev, et al. 2008) (Figure 2.1). The second base makes a stacking interaction with His 193/203, while the third base rearranges and stacks on G530 of 16S rRNA. Unstacking of the third base distorts the mRNA backbone causing A1492 of 16S rRNA to move out from helix 44 and contact the mRNA backbone. Movement of A1492 opens up space for A1913 of 23S rRNA to stack with A1493 of 16S rRNA. Without these conformational changes, A1913 would block binding of RFs. Thus, His 193/203 seems to play a key role in switching the conformation of the ribosome to a state that is productive for RF1/2 binding and peptide release. Here we analyzed the functional importance of the conserved His 197 in RF1 of *E. coli* (corresponding to His 193 and His 203 of *T. thermophilus* RF1 and RF2, respectively) using equilibrium binding studies, transient-state kinetic methods and peptide release assays. Our results show that His 197 in RF1 is critical for stably binding the release factor to the ribosome and for efficient peptide release.

RESULTS

Equilibrium binding of H197A RF1 to ribosome

To study the functional role of the highly conserved histidine at position 197 in *E. coli* RF1, we changed it to an alanine by site-directed mutagenesis.

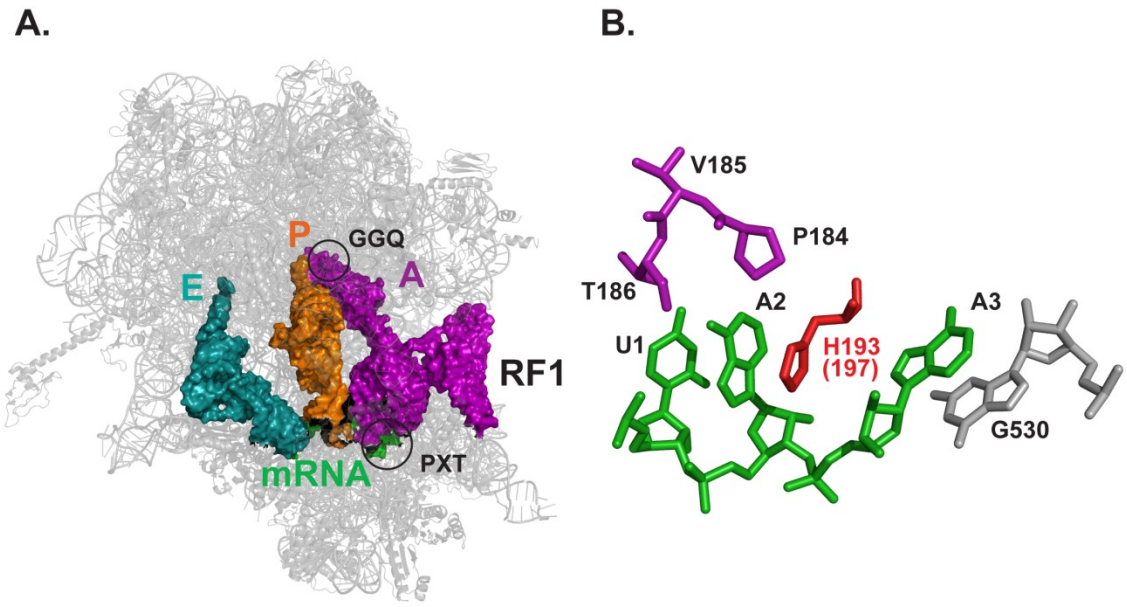

Figure 2.1: Structure of RF1 bound to the ribosome. (A) Location of RF1 in the ribosome: ribosome (gray), RF1 (purple), P site tRNA (orange), E site tRNA (teal) and mRNA (green). Circles indicate the highly conserved GGQ and PXT loops. (B) Close-up of the interactions between RF1 and the stop codon: RF1 residues (purple), stop codon $U_1A_2A_3$ (green) and G530 of 16S rRNA (grey). *T. thermophilus* numbering is used for the RF1 residues except for His 193 (red) where the corresponding *E. coli* residue His 197 is indicated. The structure figures were prepared using PyMol. Protein Data Bank ID 3D5A and 3D5B (Laurberg, et al. 2008).

Wild type and H197A RF1 were purified and then were analyzed for their ability to bind to ribosomes using a recently described fluorescence-based assay (Hetrick, Lee and Joseph 2009). Release complexes (RC) were formed by sequentially adding pyrene-labeled mRNA and $tRNA^{fMet}$ to 70S ribosomes. Binding of $tRNA^{fMet}$ to the P site positions the UAA stop codon in the A site. Increasing amounts of wild type or H197A RF1 were added to a fixed concentration of RC. The increase in fluorescence emission intensity due to RF1 binding to the RC was measured for each concentration of RF1. As reported previously, the affinity of wild type RF1 for a UAA stop codon is very high (Hetrick, Lee and Joseph 2009). For sufficient signal over noise, the minimum concentration of RC required for the titration experiment is 5 nM, which is close to the K_D of the wild type RF1 binding to the ribosome hence, the K_D could not be accurately determined for wild type RF1; our best estimate is that it is below 3 nM (Figure 2.2). In contrast, H197A RF1 showed at least a 100-fold increase in the K_D compared to wild type RF1 (K_D = 350 ± 30 nM). Thus, histidine 197 of RF1 is essential for binding to the ribosome with high-affinity.

Kinetics of H197A RF1 binding to ribosome

To determine the rates of stop codon recognition by RF1, we studied the transient-state kinetics of H197A RF1 binding to RC. Time courses of RF1 binding to RC were determined using a stopped-flow instrument (Figure 2.3A). A biphasic increase in fluorescence was observed when both wild type and H197A

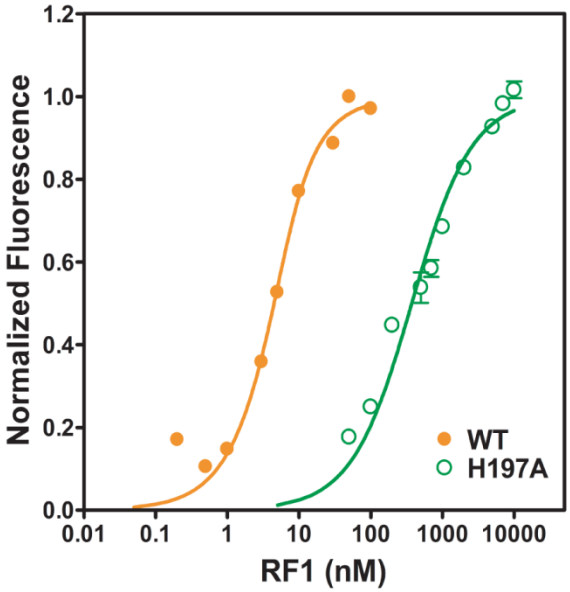

Figure 2.2: Fluorescence assay for determining the K_D of H197A RF1. Normalized changes in fluorescence intensity after adding increasing concentrations of wild type RF1 (orange) or H197A RF1 (green) are shown. A representative titration experiment for wild type RF1 without standard deviations is shown. The standard deviations from four independent experiments are shown for H197A RF1. The curves shown are fit to the quadratic equation.

RF1 bind to RC. Previously, the fluorescence change observed when wild type RF1 bound to RC was described as having only a single phase (Hetrick, Lee and Joseph 2009). This previous data was analyzed up to six half-lives and fit well to a single exponential equation however, our analysis of longer time courses revealed a second, slower phase. The simplest interpretation of the biphasic kinetic data is a two-step binding process (Johnson 1992). The first phase is likely a second order association step and the second phase a conformational rearrangement of the complex. The observed rates of each phase of the fluorescence change were determined by fitting stopped-flow time courses to a double exponential equation. A plot of the observed rate of the first phase of the fluorescence change versus RF1 concentration revealed a linear concentration dependence, consistent with a second order association step (Johnson 1992) (Figure 2.3B). The slope of the line is the second order association rate constant of RF1 for the ribosome (k_1). Wild type and H197A RF1 bind to the ribosome with nearly identical association rate constants of 55 μM^{-1} s^{-1} and 71 μM^{-1} s^{-1}, respectively. Therefore, the association rate constant (k_1) of RF1 binding to the ribosome was unaffected by the H197A mutation.

The dissociation rate constant (k_{-1}) was obtained from the y-intercept of the concentration dependence plot of phase 1 (Johnson 1992) (Figure 2.3B). The k_{-1} value for wild type RF1 is very small and cannot be accurately determined, which is consistent with an equilibrium K_D of less than 3 nM. Interestingly, the k_{-1} value for H197A is 175 s^{-1}, indicating that it forms an initial labile complex with the ribosome compared to wild type RF1. The K_{D1} for H197A

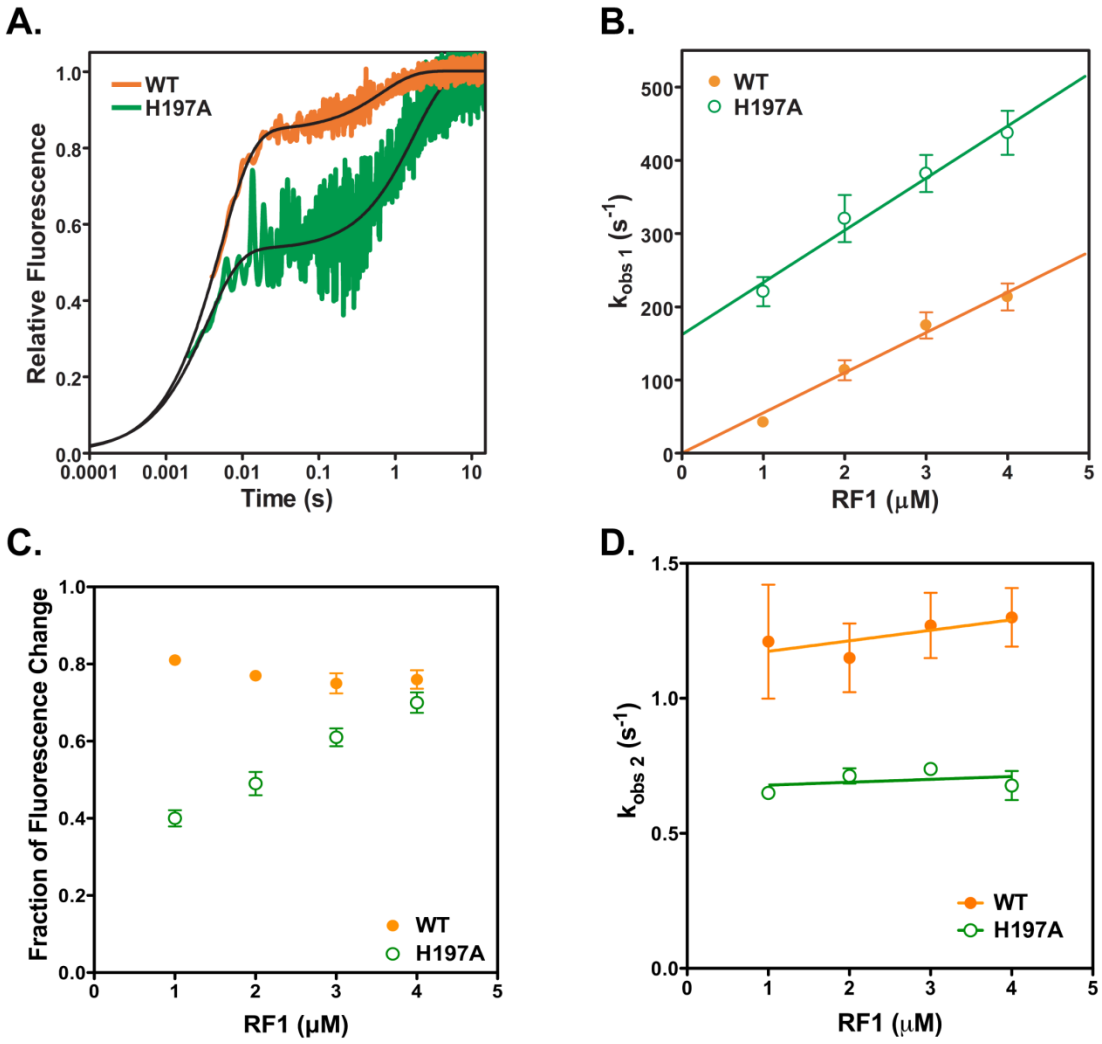

Figure 2.3: Kinetics of H197A RF1 binding to the ribosome. (A) Representative stopped-flow time course of wild type RF1 (orange trace) and H197A RF1 (green trace) binding to ribosome. The time courses were fit to a double-exponential equation (black line) to determine the observed rates of RF1 binding (k_{obs1} and k_{obs2}). (B) Concentration dependence of the *observed rate* for phase 1 of RF1 binding. Plots were fit to a linear equation to determine the association (k_1) and dissociation (k_{-1}) rate constants. (C) Concentration dependence of the *amplitude* for phase 1 of RF1 binding. (D) Concentration dependence of the observed rate for phase 2 of RF1 binding. Plots were fit to a linear equation. In all cases, the standard errors from at least three independent experiments are shown.

binding to the RC calculated from the k_1 and k_{-1} values is 3 μM. This value is 10-fold higher than the equilibrium K_D determined from the titration experiments described above (K_D = 0.35 ± 0.03 μM). This suggests that the initial labile complex formed by H197A on the ribosome undergoes a conformational change over time to a more stable complex further indicating a two step binding process. Examination of the amplitudes for phase 1 is also consistent with this interpretation. The amplitude for phase 1 did not change with increasing concentrations of wild type RF1 showing that binding has been saturated (Figure 2.3C), which matches the < 3 nM K_D for wild type RF1. In contrast, the amplitude for phase 1 increased with increasing concentrations of H197A RF1 showing that saturation has not been reached at the lower concentrations (Figure 2.3C). The half maximal change in amplitude is observed at 2-3 μM of H197A RF1, which agrees with the calculated K_{D1} of 3 μM from phase 1. These results show that H197A mutation in RF1 significantly reduces the stability of the initial complex formed on the ribosome.

The dissociation rate constant (k_{-1}) was obtained from the y-intercept of the concentration dependence plot of phase 1 (*16*) (Figure 2.3B). The k_{-1} value for wild type RF1 is very small and cannot be accurately determined, which is consistent with an equilibrium K_D of less than 3 nM. Interestingly, the k_{-1} value for H197A is 175 s^{-1}, indicating that it forms an initial labile complex with the ribosome compared to wild type RF1. The K_{D1} for H197A binding to the RC calculated from the k_1 and k_{-1} values is 3 μM. This value is 10-fold higher than the equilibrium K_D determined from the titration experiments described above (K_D

= 0.35 ± 0.03 μM). This suggests that the initial labile complex formed by H197A on the ribosome undergoes a conformational change over time to a more stable complex further indicating a two step binding process. Examination of the amplitudes for phase 1 is also consistent with this interpretation. The amplitude for phase 1 did not change with increasing concentrations of wild type RF1 showing that binding has been saturated (Figure 2.3C), which matches the < 3 nM K_D for wild type RF1. In contrast, the amplitude for phase 1 increased with increasing concentrations of H197A RF1 showing that saturation has not been reached at the lower concentrations (Figure 2.3C). The half maximal change in amplitude is observed at 2-3 μM of H197A RF1, which agrees with the calculated K_{D1} of 3 μM from phase 1. These results show that H197A mutation in RF1 significantly reduces the stability of the initial complex formed on the ribosome.

The observed rates of the second phase of the fluorescence change did not vary with the concentration of RF1 for both wild type and H197A (Figure 2.3D). The lack of concentration dependence is consistent with a first order conformational change after binding (Johnson 1992). The rate of the second phase of the fluorescence change is saturated at 1.3 s^{-1} for wild type RF1 and somewhat more slowly at 0.7 s^{-1} for H197A RF1. Since the rates for the second phase are similar it means that H197 is not critical for this conformational change to occur after the initial binding step. However, H197 is required for the stability of the complex in the second phase because the equilibrium K_D for the H197A RF1 is at least 100-fold higher than wild type RF1. Thus, equilibrium binding studies and kinetic analysis reveal that H197 is critical for the initial binding step

and for the overall stability of RF1 in its finally bound conformation on the ribosome.

Kinetics of peptide hydrolysis by H197A RF1

To investigate whether histidine 197 of RF1 is important for the catalytic step, the rate of peptide release by H197A RF1 was determined. Release complexes were formed by binding [S^{35}]fMet-$tRNA^{fMet}$ to the P site. Peptide release time courses were performed by adding saturating amounts of RF1 (20 μM, which is more than 50-fold above the K_D for H197A RF1 binding to RC). RF1-catalyzed release of [S^{35}]fMet was analyzed by electrophoretic TLC and quantitated with a phosphorimager. To verify that saturation was reached, the time courses were repeated with double the concentration of RF1 and identical time courses were obtained. Wild type RF1 catalyzed peptide release with a rate of 0.25 ± 0.02 s^{-1}, which is consistent with previously published data (Hetrick, Lee and Joseph 2009; Youngman, et al. 2007). In contrast, H197A RF1 showed a ≈5-fold reduced rate of peptide release ($k_{release}$ = 0.053 ± 0.004 s^{-1}). The reduced catalytic activity of H197A RF1, even under saturating concentrations, can be explained by a misalignment of the mutant RF1 in the ribosome, which may affect the positioning of the universally conserved GGQ loop in the peptidyl transferase center.

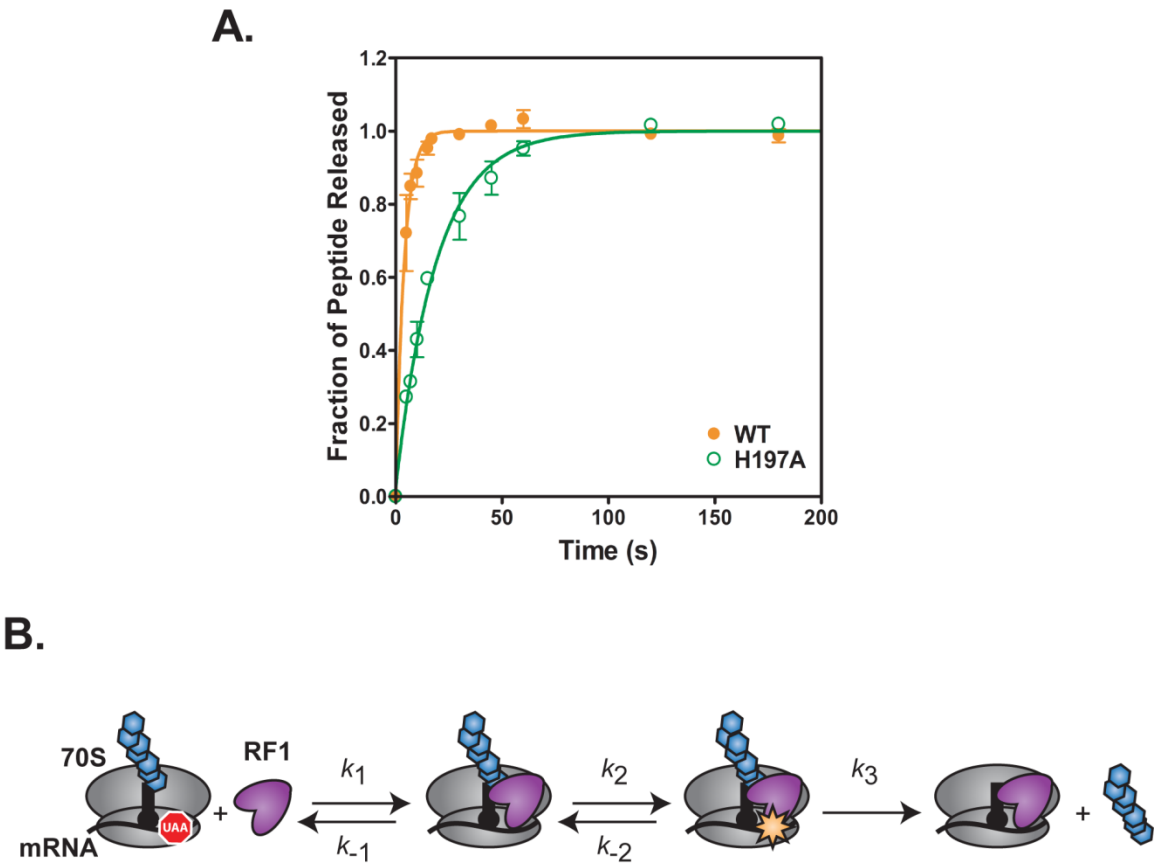

Figure 2.4: Peptide release time course and a schematic model for RF1 binding and peptide release. (A) Peptide release time courses at saturating concentrations of wild type RF1 (orange circles) and H197A RF1 (green circles). Data were normalized and fit to a single-exponential equation (line) to determine the rate of peptide release. (B) Cartoon showing the kinetic steps in RF1 binding to the ribosome and catalyzing peptide release. Ribosome (grey), stop codon (red), P site tRNA (black stem loop), polypeptide (blue hexagons) and RF1 (purple). Step 1 is the second-order association step of RF1 to the ribosome (k_1, k_{-1}). Step 2 is a first-order conformational switch to a more tightly bound complex (k_2, k_{-2}). Step 3 is the peptidyl-tRNA hydrolysis reaction catalyzed by RF1 (k_3).

Discussion

Stop codon recognition by RFs is essential for the correct termination of protein synthesis in all organisms. Recent crystallographic structures have revealed the interactions between conserved residues in the RFs and the stop codon in the decoding center that are important for discrimination (Laurberg, et al. 2008; Wiexlbaumer, et al. 2008). These structures have also made it possible to perform molecular dynamics simulations to understand the energetics of stop codon recognition (Sund, Ander and Aqvist 2010). Nevertheless, the contribution of critical residues in the RF to binding, conformational changes, and catalysis has to be determined experimentally to fully understand the mechanism of stop codon recognition.

In this study, we focused on the highly conserved His 197 in *E. coli* RF1 that seems to play a central role in triggering conformational changes in the decoding center. We made use of a recently developed fluorescence-based, transient-state kinetic method (Hetrick, Lee and Joseph 2009) to quantitatively evaluate the role of His 197 in stop codon recognition and in the catalysis of peptide release. Equilibrium binding studies showed that H197A RF1 has a drastically larger K_D that is 100-fold over the wild type RF1 (Figure 2.2).

The transient-state kinetics of RF1 binding showed a biphasic fluorescence change and, with the concentration dependence profiles described above, can be interpreted as a second order association step followed by a first order conformational change (Johnson 1992). However, other binding

mechanisms may also result in biphasic kinetics such as subpopulations of either binding partner or multiple binding pathways. But analysis of the concentration dependence of the amplitudes of each phase of the fluorescence change associated with wild type RF1 binding to the ribosome supports the two step binding mechanism over these other mechanisms.

The kinetic data show that the association rate constants (k_1) are similar for wild type and H197A RF1. By contrast, the dissociation rate constant is at least 1000-fold faster for H197A RF1 (k_{-1} < 0. 1 s^{-1} for wild type RF1 and k_{-1} = 175 s^{-1} for H197A RF1) (Figure 2.3). Interestingly, the dissociation rate constant of H197A RF1 is similar to the value obtained with wild type RF1 binding to a sense codon in the decoding center (k_{-1} = 25-350 s^{-1}) (Hetrick, Lee and Joseph 2009). His 197 in RF1, therefore, is clearly essential for the initial binding interaction with the ribosome. It is possible that the stacking interaction of the second base of the stop codon with His 197 triggers conformational changes in the decoding center that locks the RF on the ribosome.

The time course of RF1 binding to the ribosome showed a second, slow phase that is independent of the concentration of RF1. This is consistent with a first order conformational change following the RF1 association step. The rates for the second phase (k_2) are similar for wild type and H197A RF1 indicating that H197 is not essential for this conformational change. The saturation rate of 1 s^{-1} for the second phase is comparable to the rate of peptide release by RF1 suggesting that it is on the reaction coordinate leading to catalysis ("on-pathway"). The second phase may be monitoring the switch into the more tightly

bound final conformation. However, the final conformation attained by H197A RF1 has a 100-fold lower binding affinity compared to wild type RF1. This can be partially explained by the loss of favorable stacking interactions with the second base of the stop codon, the inhibition of conformational changes in the decoding center that overcomes the steric clash by A1913 of 23S rRNA, the global misalignment of H197A RF1 on the ribosome or a combination of these factors.

The rate of peptide release is 5-fold slower with H197A RF1 compared to wild type RF1 (Figure 2.4A). This lower rate of peptide release is not due to decreased binding of H197A RF1 because these experiments were performed with saturating amounts of H197A RF1. The most likely explanation is that H197A RF1 is not correctly bound to the decoding center of the ribosome. This may cause the rest of the H197A RF1 to become misaligned, especially the universally conserved GGQ motif that is essential for peptide release. Indeed, recent structure probing studies have shown that a sense codon in the decoding center can cause RF1 to become incorrectly positioned in the ribosome (He and Green 2010). However, the rate of peptide release is inhibited by 100–1000-fold with a sense codon (Hetrick, Lee and Joseph 2009) indicating that the overall arrangement of H197A RF1 on the ribosome is still somewhat similar to the wild type RF.

In summary, our studies quantitatively evaluated the role of the highly conserved H197 in RF1 binding to the ribosome and the catalysis of peptide release. Our results show that H197 is critical for the binding step and significant

for peptidyl-tRNA hydrolysis. In addition, we show that after the initial binding step by H197A RF1 to the ribosome, a conformational switch occurs to a more tightly bound state (Figure 2.4B). Quantitatively determining the role of other residues in RF1/2 for stop codon recognition and catalysis of peptide release is essential for mechanistically understanding how these protein factors achieve their high-fidelity during translation termination.

Chapter 2 is reproduced with permission from Field, A.; Hetrick, B.; Mathew, M.; and Joseph, S. (2010) Histidine 197 in release factor 1 is essential for A-site binding and peptide release, pending publication in *Biochemistry*, submitted July 29, 2010.

Chapter 3: RF3 Nucleotide Dependence

Introduction

Prokaryotic RF3 is responsible for the rapid dissociation of class I release factors after peptide release (Freistroffer, et al. 1997; Zavialov, Buckingham and Ehrenberg 2001). RF3 is a known GTPase and utilizes guanine nucleotides to fulfill its catalytic function (Grentzmann, et al. 1998). A mechanism has been proposed in which the exchange of guanine nucleotides by RF3 on the ribosome triggers a large scale conformational change in both the ribosome and the release factor itself resulting in RF1 or RF2 dissociation (Figure 1.5) (Zavialov, Buckingham and Ehrenberg 2001; Zavialov, Mora, et al. 2002). The hydrolysis of GTP after this event allows for RF3 to leave the RC (Zavialov, Buckingham and Ehrenberg 2001; Zavialov, Mora, et al. 2002).

These conclusions were drawn, in large part, from peptide release assays that utilized the turnover of limiting concentrations of class I release factors (Zavialov, Buckingham and Ehrenberg 2001; Zavialov, Mora, et al. 2002). Release complexes were created with 70S ribosomes, labeled tetrapeptide-tRNA in the P-site, and a vacant A-site programmed with a stop codon. A limiting amount of RF2 was then added to these complexes and allowed to bind. Tight binding of the class I release factor ensured minimal background turnover. RF3 was then required to free RF2 to allow binding to another RC to then catalyze the

release of more tetrapeptide. RF2 was introduced in such limiting quantities that multiple turnovers were necessary to completely hydrolyze all tRNA-bound tetrapeptides. The rate of peptide release would then serve as an approximation of the release of RF2, but the release event was never directly observed. With this assay, RF3-GTP and an excess of RF3 with GDPNP, a non-cleavable GTP analog, were found to strongly stimulate peptide release indicating large turnover of RF2.

The proposed conformational change upon GDP exchange for GTP is evidenced by cryo-EM structures of RF3-GDPNP bound to RC (Klaholz, Myasnikov and Van Heel 2004). Release complexes were evenly distributed between two distinct structural states. The first state exhibited a structure similar to RF3-GDP bound to the ribosome in which the A-site remained open and the tRNA still resided in the P-site. The second state, however, showed a large scale conformational change, similar to translocation. The ribosomal subunits rotated approximately six degrees with respect to each other, the P-site tRNA transitioned to the E-site, and the decoding center was distorted (Agrawal, et al. 1999; Stark, et al. 2000; Klaholz, Myasnikove and Van Heel 2004). The authors cited these two states as evidence that the GTP binding event causes the conformational change required to eject class I release factors due to the distortion of the A-site. However, these release complexes were formed without the use of a class I release factor and the nascent peptides were artificially removed with puromycin. If a class I release factor was present in the A-site, it is

unclear whether the second state conformation could be adopted with just GTP binding.

Here we investigate a new way of observing RF3 catalysis by directly measuring the decoding center interaction of RF1via a fluorescent mRNA probe (Hetrick, Lee and Joseph 2009). This method has the potential of gathering accurate measurement of the kinetics involved with RF3 mediated class I release factor ejection and may also serve to validate or amend the adopted mechanism.

Results

RF3 trap experiments

The fluorescence-based approach for RF1 binding used in chapter 2 was adapted for use with RF3. Pyrene labeled mRNA with a stop codon programmed in the A-site of release complexes was used as a substrate for RF1. Binding of RF1 again produced a fluorescence increase as observed previously (Figure 3.1) (Hetrick, Lee and Joseph 2009). Direct addition of His-tagged RF3 and the nucleotides GDP, GTP and GDPNP to the reaction mixture, however, yielded no significant change in fluorescence (Figure 3.1). This could possibly be caused by the immediate rebinding of RF1 to RC, the assay is insensitive to RF1 release or the RF3 is inactive.

To test for the possibility of RF1 rebinding, a trap experiment was devised (Figure 3.2). Pyrene labeled RC (RC*) was preincubated with RF1 then mixed

with 5-fold excess unlabeled RC which was similarly programmed with a stop codon in the empty A-site. If RF3 actively ejects RF1, the RF1 would more likely rebind to the unlabeled complexes hence reducing the overall fluorescence signal intensity. Experiments using this method did show a dramatic decrease in fluorescent signal with GTP and RF3 but under no other conditions. This suggests that GTP hydrolysis may be necessary for RF3 catalysis.

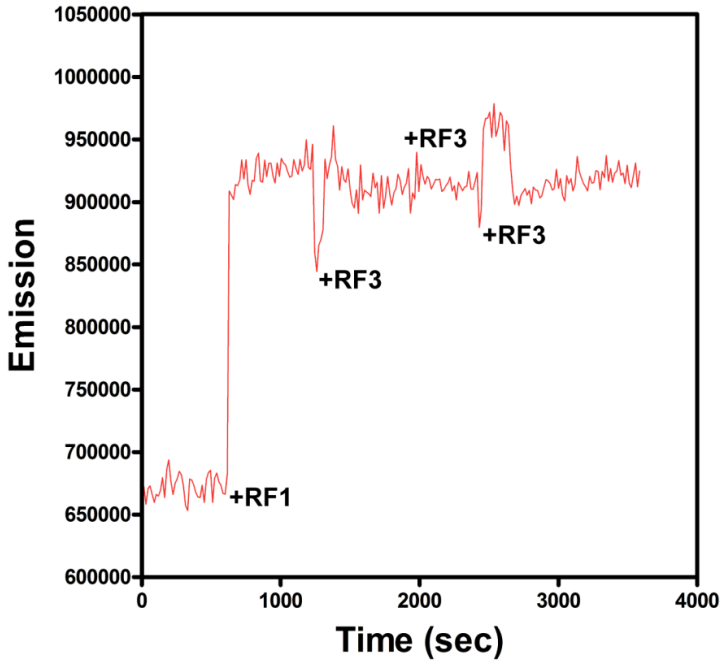

Figure 3.1: Initial RF3 fluorescence time scans. Above shows the initial time scan of release complex with His-tagged RF3 and GTP. A large increase of fluorescence was observed when RF1 was added at 600 seconds. When additions of RF3 and GTP (2-fold over RC concentration) were made as indicated on the plot at 1200 seconds, 1800 seconds and 2400 seconds, no significant change in signal was observed. The slight variance seen above can be attributed to mixing of the solution after each addition or dilution. Similar results were obtained for GDP, GDPNP, and no added nucleotides (not shown).

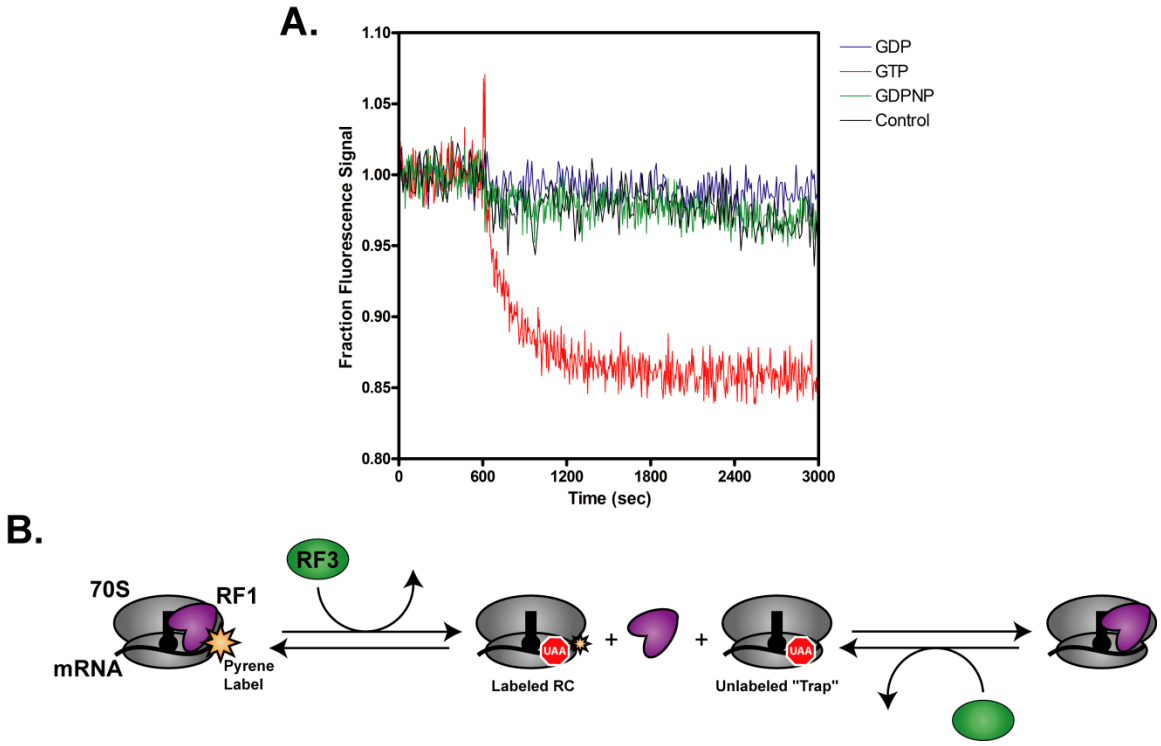

Figure 3.2: RF3 trap experiments. (A) RF3 was added at 600 seconds for all samples with GDP (blue), GTP (red), GDPNP (green), and no trap ribosomes (black). No significant change (< 5%) was observed for experiments with GDP, GDPNP, and no trap, but a drastic decrease (~15%) in fluorescence was observed for GTP indicating release of RF1. Similar results were obtained for both His-tagged and intein-tag purified RF3 (intein-tag purified shown). (B) A scheme of the RF3 mediated reaction is shown. Ribosome (grey), stop codon (red), P-site tRNA (black stem loop), RF3 (green) and RF1 (purple). Preincubated labeled RC with RF1 begins on the left. As RF3 reacts with the labeled RC, RF1 is released and is free to bind with the unlabeled trap. With the progression of time, the equilibrium will shift to the right as the excess unlabeled RC is occupied by the released RF1 and signal decreases.

Equilibrium binding of RF3 with excess guanine nucleotides

Surprisingly, the trap experiments showed no sign RF1 ejection with GDPNP which is contrary to previous results with turnover experiments (Zavialov, Buckingham and Ehrenberg 2001; Zavialov, Mora, et al. 2002). This, however, does not mean binding of RF3 is not loosened when GDPNP is present. To examine a possible change in binding affinity, the K_D of RF1 was measured in the presence of RF3 and a large excess of guanine nucleotides as described in chapter 4 (Figure 3.3). Only RF3 with GTP showed a significant increase in RF1 K_D at 50 nM. RF3 with GDP, GDPNP and no nucleotide fell close to or below the measureable threshold for signal over noise of 5 nM. The highest approximated K_D out of these conditions was for GDPNP at 6 nM, but this is not significantly higher than RF1 alone (approximately 2 – 3 nM). Although this data is not conclusive, it would seem that no significant loss of binding occurs without GTP hydrolysis.

GTP hydrolysis

As a check of the activity of the His-tagged RF3, a GTP hydrolysis assay was preformed (Figure 3.4). The conditions of previous experiments were mimicked as outlined in chapter 4 (Zavialov, Buckingham and Ehrenberg 2001). Surprisingly, the His-tagged RF3 showed no increase in the rate GTP hydrolysis

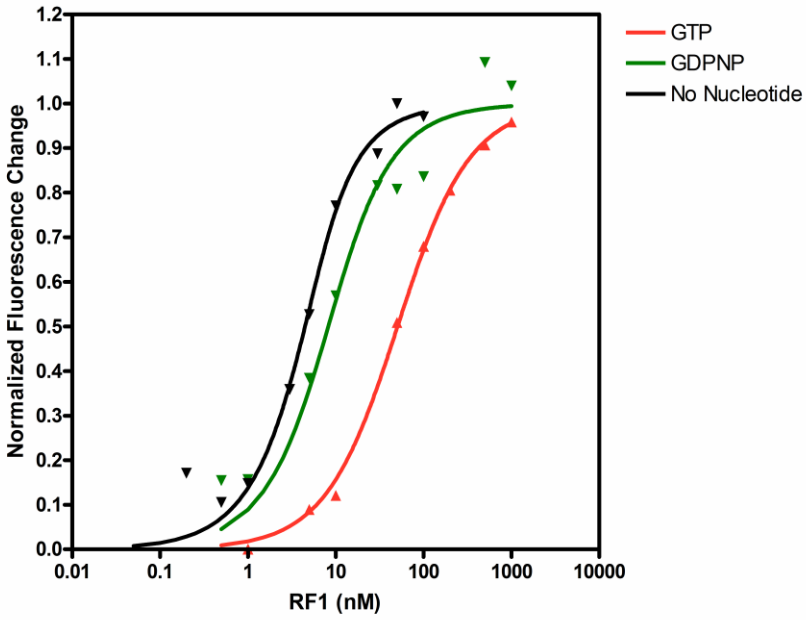

Figure 3.3: RF1 K_D with RF3 and nucleotides. Above the K_D data is shown for RF1 in the presence of His-tagged RF3 and the indicated nucleotides. RF3-GTP (red), RF3-GDPNP (green) and RF3 with no added nucleotide (black). With RF3-GTP, RF1 has a ten-fold higher K_D than without nucleotides. Within the limitations of the assay, RF1 with RF3-GDPNP shows a similar K_D to no nucleotide. RF3 with no nucleotide produced a K_D below 5 nM. GDP (not shown) also produced a K_D below the measurable threshold.

over the basal ribosomal rate. All reactions consistently hydrolyzed approximately 15-20% of the initial GTP after 30 minutes. Since other sources have reported complete hydrolysis under these conditions within 10 minutes (Zavialov, Buckingham and Ehrenberg 2001), a new purification technique was used to procure untagged RF3 (intein-tag samples). However, even this newly purified RF3 produced identical results in both trap experiments and GTP hydrolysis (Figure 3.2 and Figure 3.4). The RF3 expression plasmid was also sequenced, but no errors were found.

Discussion

In this chapter, we examined the nucleotide dependence of RF3 catalysis via fluorescence based assays for RF1 binding. Preliminary trap experiments seemed promising with RF3-GTP leading to a drastic fluorescence change that stabilized after about ten minutes in all trials. Curiously, GDPNP did not have the same effect. Previous studies have linked the exchange of GDP for GTP on the ribosome as cause of a conformational change leading to RF1 ejection (Zavialov, Buckingham and Ehrenberg 2001; Zavialov, Mora, et al. 2002). This was evidenced by a dramatic increase in peptide release in turnover experiments with excess RF3 and GDPNP. However, we found no evidence that such an event could be caused by class I release factor recycling with RF3-GDPNP.

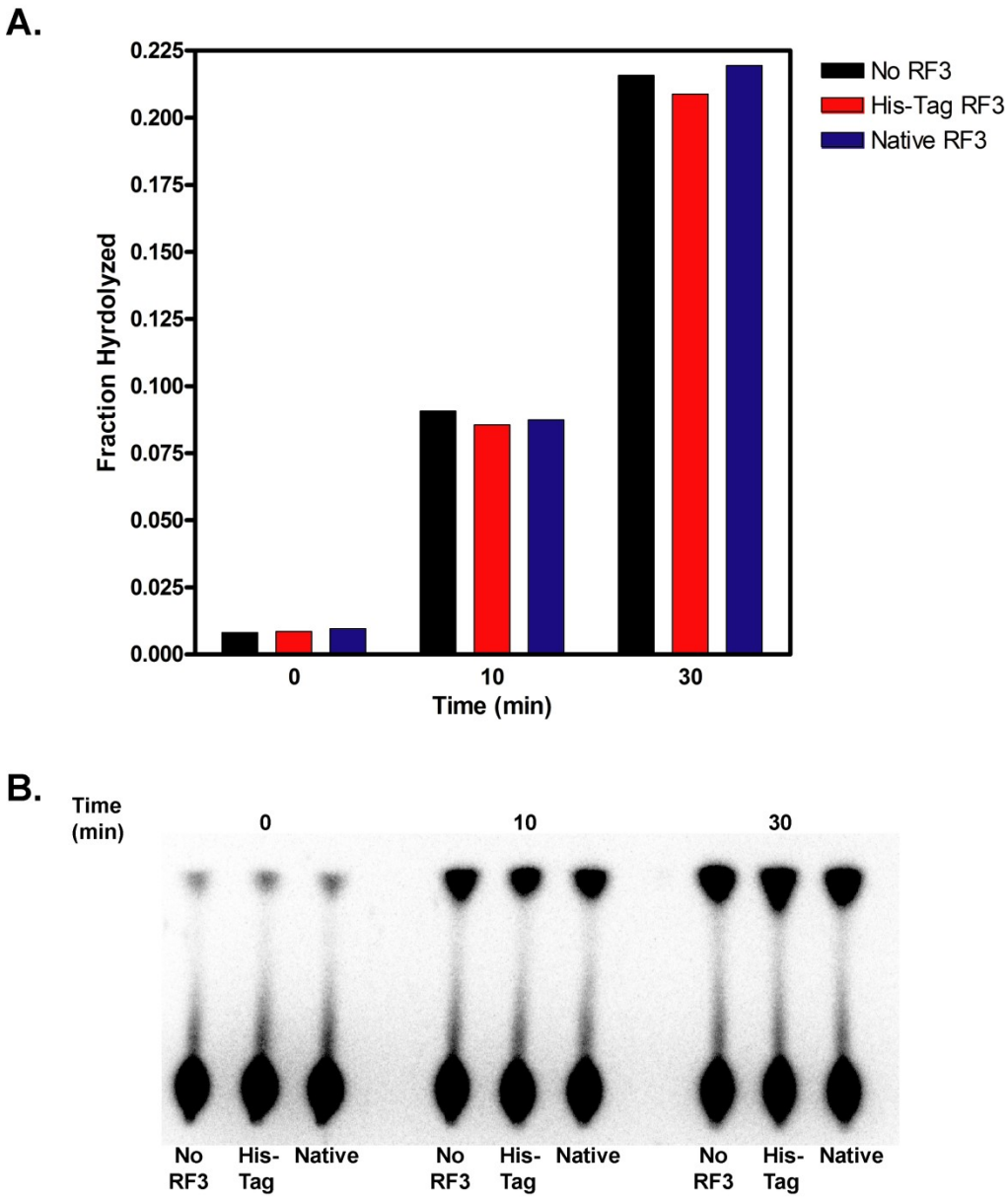

Figure 3.4: RF3 GTP hydrolysis. (A) A representative time course of the fraction of hydrolyzed GTP by RF3 and RC with RF1 bound. All RF3 purifications produced virtually identical time courses over 30 minutes which matched the basal ribosomal levels. (B) An example of a TLC used in a hydrolysis time course. RC alone (No RF3), His-tagged RF3 (His-Tag) and native RF3 (Native) are shown at three time points. The top band represents the hydrolyzed GTP and the bottom band is the unhydrolyzed portion.

In addition, binding experiments revealed a ten-fold increase in the approximate K_D of RF1 with RF3 and GTP. This is a significant loosening of the RF1 interaction in the decoding center and is consistent with the release seen in preliminary trap experiments. Although the measurements of K_D reached the lower limit of concentration allowed by our signal thus not yielding accurate measurement, GDPNP still seemed to show an insignificant change in the K_D over RF1 alone, further indicating that GTP binding may be insufficient for the catalysis of RF1 ejection.

GTP hydrolysis, however, was unpromising for the RF3 used in these experiments. Regardless of purification method used, none of the RF3 samples increased the rate of GTP hydrolysis over the basal ribosomal rate. Previous studies have shown that with RF1 and ribosomes, RF3 significantly increases the rate of GTP hydrolysis and reaches completion under these conditions within 10 minutes (Zavialov, Buckingham and Ehrenberg 2001). This may indicate a defect in the protein being used, but analysis of the RF3 expression plasmid sequence did not reveal any errors.

Another explanation may be that the protein is inactivated or denatured during purification. For this reason, two different purification techniques were used: His-tagged and intein-tagged. Both were co-purified with GDP as well to ensure GDP was still bound to eluted proteins. Still, both purification methods produced the same results in the preliminary fluorescence experiments and GTP hydrolysis.

Even if both samples of RF3 are inactive, they still seem to show identical RF1 ejection activity with GTP and strong discrimination against GDPNP. This implies that the cleavability of GTP is important for the catalysis of release, but the protein still lacks the ability to stimulate accelerated hydrolysis under the conditions tested. It is unclear whether the activity of RF3 can be resolved using these methods.

Chapter 4: Materials and Methods

Buffers, ribosomes, tRNA, mRNA, and RF1 preparation

Experiments were performed in 20 mM Hepes-KOH (pH 7.6), 150 mM NH_4Cl, 6 mM $MgCl_2$, 4 mM β-mercaptoethanol, 2 mM spermidine, and 0.05 mM spermine (Bartetzko and Nierhaus 1988). *Escherichia coli* MRE600 were used to produce tightly-coupled 70S ribosomes as described previously (Powers and Noller 1991). mRNA with a UAA stop codon was purchased from Dharmacon and pyrene was covalently attached as described before (Studer, Feinberg and Joseph 2003). Native $tRNA^{fmet}$ was purchased from Sigma. His-tagged *E. coli* RF1 (referred to as wild type from here on) was purified as described previously (Hetrick, Lee and Joseph 2009).

Mutant H197A RF1

QuickChange (Stratagene) site-directed mutagenesis was utilized to produce the H197A RF1 mutant from the wild type RF1 plasmid. DNA primers for the mutation were purchased from ValueGene. The H197A RF1 was then sequenced, transformed into BL21 (DE3) and purified in the same manner as the wild type RF1.

RF3 purification

RF3 used in these experiments was purified in two ways. The first utilized a C-terminal His-tagged *E. coli* RF3 (plasmid was a generous gift from Kevin Wilson) and purified in much the same way as His-tagged RF1 (Hetrick, Lee and Joseph 2009) except with the addition of 30μM GDP to lysis and wash buffers, 20μM GDP to elution buffer, and 10μM GDP to the storage buffer. A C-terminal intein-tagged RF3 plasmid was also prepared from the His-tagged *E. coli* RF3 essentially as described by the IMPACT™-CN protein purification manual (New England Biolabs, Inc.). This allowed for the purification of native RF3 without a tag as described before (Feinberg and Joseph 2006). GDP was added to all buffers in the same fashion as with the His-tagged purification. An SDS-PAGE gel showing products from both purification methods is shown in Figure 4.1.

GDP purification

Commercial GDP was separated from contaminating GTP by HPLC. 3.5 mg of GDP (Sigma) was dissolved in 100 μL 20 mM of Tris-Cl, pH 7.5 (Buffer A). The GDP solution was then filtered through a Spin-X 0.2 micron filter (Corning) and loaded onto a Dionex DNA Pac PA-100 column. The column was then eluted by an increasing concentration of NaCl. Nucleotide elution was detected by absorbance at 260 nm (Figure 4.2). Fractions of GDP were pooled and precipitated by the addition of pure ethanol and incubation at -80ºC for an hour.

GDP was then pelleted by centrifugation, redissolved in water and precipitated again to remove salts. Centrifugation was repeated then the GDP pellet was dried via speed-vac, dissolved in storage buffer (25 mM Tris, 800 mM NH_4Cl, 10% acetonitrile, pH 7.5) to a concentration of 40 mM, and stored at -20ºC. All experiments requiring GDP used HPLC purified stocks.

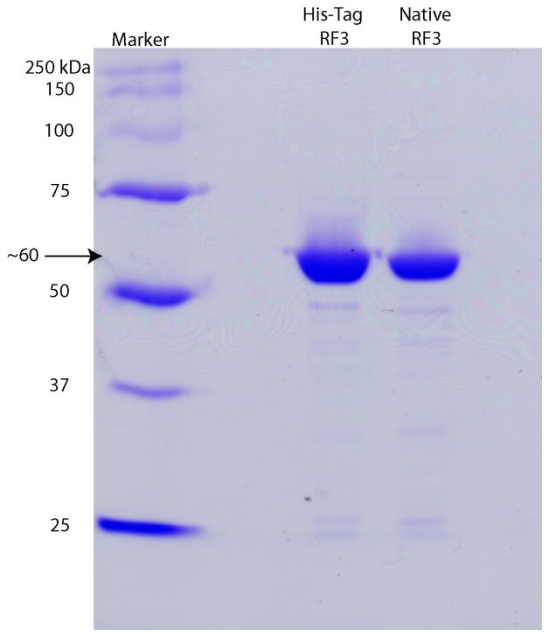

Figure 4.1: RF3 SDS-PAGE gel. Above is an SDS-PAGE gel of RF3 products from the His-Tagged (His-Tag RF3) and intein-tag (Native RF3) methods. Both protein products had a molecular weight of about 60 kDa which matches the actual value.

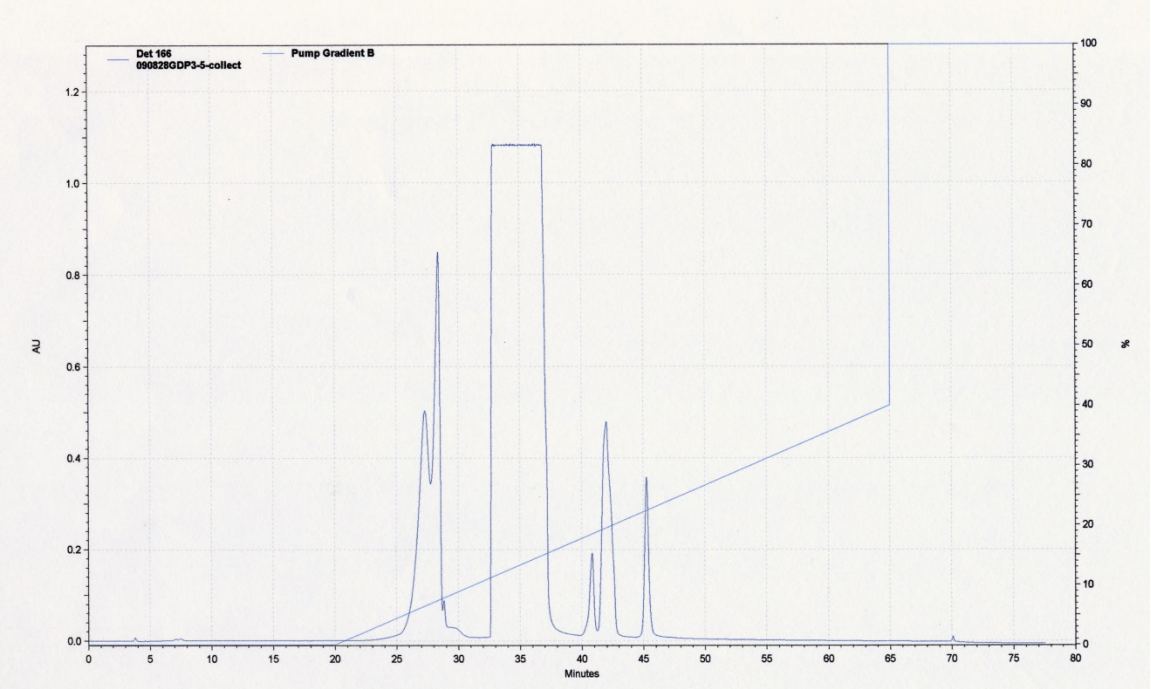

Figure 4.2: Dionex DNA Pac PA-100 HPLC GDP purification. Peaks represent the absorbance of the eluate at 260 nM with absorbance units (AU) ruled on the left vertical axis. Increasing concentration of NaCl is represented by the escalating Pump Gradient B line scaled on the right vertical axis. The second peak centered around 35 minutes represents the GDP elution and was collected for purification.

Fluorescence measurements and K_D titrations of RF1

Release complexes were formed as described before (Hetrick, Lee and Joseph 2009). The final concentration of release complex was 50 nM and 5 nM for H197A and wild type RF1 experiments, respectively. The indicated amounts of RF1 were added to the ribosome mixtures and incubated at room temperature for at least 5 minutes prior to fluorescence measurement. The fluorescence of the ribosome complexes were measured on a Fluoromax-P instrument (J. Y. Horiba, Inc.) with an excitation and emission bandpass of 1 nm, excitation

wavelength of 343 nm and the emission at 376 nm was recorded. Experiments were preformed in triplicate. Normalized emission changes were fit using Graphpad Prism using the equation below as described previously (Hetrick, Lee and Joseph 2009).

$$Y = m\{K + R + X - [(K + R + X)^2 - 4RX]^{1/2}\}/(2R)$$

where fluorescence is Y, concentration is X, the maximum fluorescence signal is m, the dissociation constant (K_D) is K, and the 70S ribosome concentration is R.

Stopped-flow binding kinetics

Stopped-flow measurements were performed essentially as described before (Hetrick, Lee and Joseph 2009). Time courses were performed with 0.25 μM release complex and the indicated amount of RF1. Data were fit to the second-order rate equation:

$$Y = b + C1*\exp(-k1*x) + C2*\exp(-k2*x)$$

where C1 and k1 are the amplitude and rate for phase 1 and C2 and k2 are the amplitude and rate for phase 2.

Peptide release assay

70S ribosomes (0.50 μM final concentration) were incubated at 42 ºC for 10 minutes then cooled to 37 ºC for 10 minutes. mRNA (1 μM final) was added to the 70S and incubated at 37 ºC for an additional 10 minutes. $tRNA^{fmet}$ was charged as described before (Hetrick, Lee and Joseph 2009) and added to the 70S-mRNA complex for a final concentration of 1.5 μM tRNA. This mixture was then incubated at 37 ºC for 30 minutes. Excess [^{35}S]Met and other unbound reaction components were removed by repeated filtration through an Amicon Ultra 100K Ultracel centrifugal filter for a final dilution of >200,000-fold. The final volume of the reaction mixture was then adjusted to a final concentration of 0.50 μM 70S ribosomes. Time courses for peptide release were carried out using 0.25 μM release complexes and 20 μM RF1 (both wild type and H197A). Each time point was quenched using 25% formic acid, run on an eTLC plate, and analyzed as described previously (Feinberg and Joseph 2006). Peptide release experiments were repeated four times.

RF3 initial fluorescence and trap experiments

Labeled release complexes were prepared as before (Hetrick, Lee and Joseph 2009). Initial experiments utilized 50 nM labeled RC with 0.5 mM nucleotides and 100 nM additions of RF1 and RF3. Fluorescence was read on a

time scan with 5-15 second intervals. RF1 and RF3 were added and mixed between the indicated time points.

For trap experiments, RF1 was added to labeled RC and allowed to incubate for 10 minutes at room temperature. Unlabeled release complexes (trap) were also prepared in the same manner but with unlabeled UAA mRNA. Trap was then added to labeled RC for a final concentration of 50 nM trap and 10 nM labeled RC. 40 nM RF3 plus 0.5 mM of GDP, GTP or GDPNP was added to labeled RC on the fluorometer and fluorescence change was recorded with 10 second time intervals.

Equilibrium binding of RF3

Dissociation contants (K_D) were measured for RF1 in the presence of RF3 and guanine nucleotides. Release complexes were formed as described previously (Hetrick, Lee and Joseph 2009). 10 nM labeled RC was used for experiments with GTP and 5 nM labeled RC was used for experiments with GDP, GDPNP or no nucleotides. All experiments had a final concentration of 0.5 nM of the indicated nucleotide (if any). For GTP experiments, RF1 concentrations were prepared separately then mixed with RC, RF3 and GTP 5 minutes prior to fluorescence measurement. The rest of the nucleotides and the experiments without nucleotides were performed by sequential addition of RF1to one reaction mixture. An approximate equilibrium was observed for each nucleotide prior to K_D measurements by extended time scan of the reaction mixture as shown in

Figure 4.3. The fluorescence of the ribosome complexes were measured on a Fluoromax-P instrument (J. Y. Horiba, Inc.) with the same parameters as before. Normalized emission changes were fit using Graphpad Prism as with the RF1 H197A mutant.

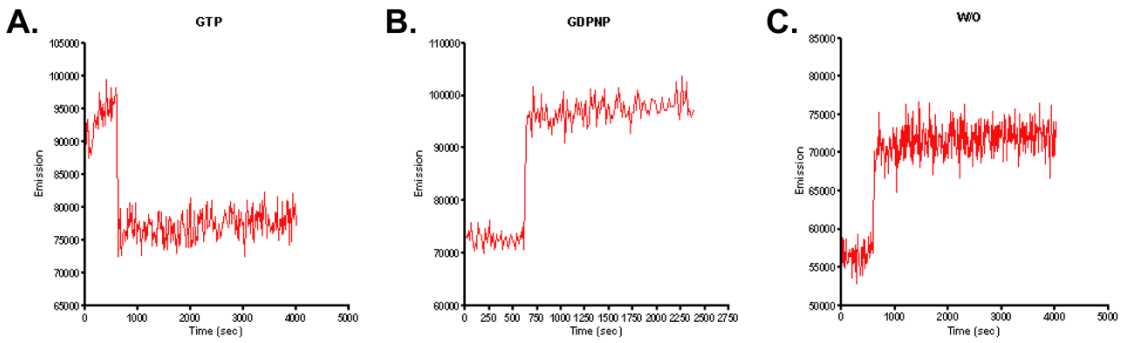

Figure 4.3: RF3 "equilibrium". The above shows three example time scans taken as preliminary data to ensure RF1 release by RF3 could be measured in an equilibrium type system. Trials with 0.5 μM GTP, GDPNP, and no nucleotide are shown in A, B, and C respectively. All three show stabilization after one minute indicating that an equilibrium-like steady state had been reached where the rate of RF1 release is equaled by the rate of binding. Similar results were also obtained in time scans of RF3 and GDP (not shown).

GTP hydrolysis

Release complexes were prepared to a final concentration of 0.25 μM. 0.5 μM RF1 was then added and allowed to bind at room temperature for 10 minutes. A mixture of 50 μM GTP (spiked with [^{32}P]GTP) and 0.5 μM RF3 (final concentrations) was then added to the RC mixture to initiate the time course. Time points were quenched with one-third volume 1.8 mM KH_2PO_4, 0.6mM $HClO_4$ and run on a TLC with 0.5M KH_2PO_4, pH 3.5 as a solvent.

Phosphoimager plates were then exposed on the dried TLCs for one hour and band density was measured on a PMI™ (Bio Rad) and calculated using Density One. The fraction hydrolyzed was calculated by the fraction of cleaved phosphate over the total phosphate and uncleaved GTP (Figure 3.4).

Chapter 4 is reproduced in part with permission from Field, A.; Hetrick, B.; Mathew, M.; and Joseph, S. (2010) Histidine 197 in release factor 1 is essential for A-site binding and peptide release, pending publication in *Biochemistry*, submitted July 29, 2010.

Chapter 5: Summary and Future Goals

Crystallography directed mutagenesis of RF1

Stop codon recognition by class I release factors is a crucial event for accurate protein synthesis. Amazingly, this process occurs by intricate decoding center interactions that do not require a proofreading mechanism (Petry, Weixlbaumer and Ramakrishnan 2008). Recent crystal structures have uncovered a multitude of previously unstudied release factor residues within close proximity to mRNA and are likely central to their function (Laurberg, et al. 2008; Wiexlbaumer, et al. 2008; Korostelev, et al. 2008).

To better understand binding and selection of stop codons by RF1, we created a mutant lacking the highly conserved histidine 197 (H197). This histidine, present in both RF1 and RF2, has been observed in crystal structures to unstack the two purines of a stop codon and promote stabilizing interactions with ribosomal RNA. With the aid of a previously developed fluorescence based assay (Hetrick, Lee and Joseph 2009), we directly measured the binding interactions in the decoding center and catalysis rates of a H197A mutant. We found that H197 is not only essential for tight binding of RF1 but also for efficient peptide release. In addition, it was observed that RF1 exhibits biphasic binding which is likely due to a two step binding mechanism: a primary labile association phase followed by tight binding in the decoding center.

To further understand the decoding process by RF1 or RF2, more mutational studies like this one could be performed on other residues observed in crystal structures (Figure 1.4) (Laurberg, et al. 2008; Wiexlbaumer, et al. 2008; Korostelev, et al. 2008). Gly116 interacts with the first position uracil (Figure 1.4A) (*Thermus Thermophilus* numbering). Glu119 stabilizes interactions in both the first and second positions of the stop codon (Figure 1.4A and B). Finally, Gln181 and Thr194 exhibit flexibility in the third codon position accepting either a G or an A (Figure 1.4C). Replacement of any of these conserved residues could provide insight into their role in binding.

In addition, computational studies have suggested that Arg182 is responsible for withdrawing Glu119 (Sund, Ander and Aqvist 2010). A similar glutamic acid in RF2, Glu128, allows for a guanine in the second codon position by a "switch" mechanism that is restricted by the arginine in RF1. Removal of this arginine may result in loss of specificity stop codon specificity.

RF3 mechanistic studies

Due to their intricate interactions, class I release factors bind tightly to the A-site following the end of elongation (Hetrick, Lee and Joseph 2009). For this reason, a class II release factor (RF3 in prokaryotes) is essential to catalyze the removal of RF1 or RF2 after peptide release (Freistroffer, et al. 1997; Zavialov, Buckingham and Ehrenberg 2001). RF3 utilizes GTP to catalyze class I release factor ejection, however, some experimental results have been contradictory

(Grentzmann, et al. 1998). A mechanism has been proposed in which the exchange of guanine nucleotides triggers a conformational change which is responsible for RF3 catalysis (Zavialov, Buckingham and Ehrenberg 2001; Zavialov, Mora, et al. 2002), but the process of RF1 or RF2 release has never been observed directly.

Here, we attempted to design an assay adapted from fluorescence based RF1 binding studies (Hetrick, Lee and Joseph 2009). This method can directly detect RF1 interaction in the decoding center and has the potential to provide accurate measurement of kinetic information. A trap experiment was devised by preincubating labeled release complexes with RF1 and stimulating release with RF3 and guanine nucleotides in the presence of excess unlabeled "trap" ribosomes. As RF1 was ejected from labeled ribosomes, it would rebind to unlabeled ribosomes resulting in signal decrease. Release of the class I RF was observed only with GTP present indicating hydrolysis was necessary for RF3 catalysis. Similarly, RF1 K_D was also measured in the presence of RF3 and nucleotides. It was found that only GTP made a significant difference to RF1 binding affinity agreeing with the trap results. These experiments, however, contradicted earlier results that seemed to suggest class I RF release with nucleotide exchange (Zavialov, Buckingham and Ehrenberg 2001; Zavialov, Mora, et al. 2002).

To confirm the activity of the RF3 used in these experiments, the rate of GTP hydrolysis was measured. Unfortunately, no hydrolysis above basal

ribosomal levels was observed suggesting a defect in the protein. Despite alternate RF3 purification methods, increased GTPase activity was not observed.

Future experiments may include repeating class I RF turnover assays to attempt to replicate the results observed in other studies (Zavialov, Buckingham and Ehrenberg 2001). If peptide release is still observed with the RF3 purified in this study and GDPNP, it may suggest that other factors influence the rates seen in the assay. Nucleotide exchange experiments may also help indicate whether there is a defect in the function of the RF3 used. Finally, if it is determined that there is a problem with the protein itself, new purification techniques may need to be employed.

Pyrene labeled mRNA fluorescence assay

Overall, pyrene labeled mRNA has proved an invaluable tool in measuring decoding center interactions for both equilibrium binding and transient-state kinetic analysis. It has allowed for evaluation of the importance of H197 in RF1 stop codon recognition and A-site binding as well as provided possibilities to assess the functional requirements of RF3. However, there do seem to be significant limitations to the use of this method. The K_D of wild type RF1, without interference from RF3 and GTP, is too low to measure accurately with the pyrene fluorescence signal. Also, the concentrations of ribosomes necessary for a trap to measure accurate transient-state kinetics of RF1 dissociation are too high for routine use. Finally, a true K_D cannot be measured for RF1 in the presence of

RF3-GTP because it is an active process that is not at a true equilibrium but a steady state. GTP is actively being hydrolyzed by the ribosome even if RF3 GTP hydrolysis is hindered. Even still, this method retains utility as an accurate measure of RF1 binding and a qualitative tool for RF3 functionality.

References

Agrawal, R. K., A. B. Heagle, P. Penczek, R. A. Grassucci, and J. Frank (1999). "EF-G-dependent GTP hydrolysis induces translocation accompanied by large conformational changes in the 70S ribosome." Nature Struct Biol **6**: 643-647.

Ban, N., P. Nissen, J. Hansen, P. B. Moore, and T. A. Steitz (2000). "The complete atomic structure of the large ribosomal subunit at 2.4 A resolution." Science **289**(5481): 905-920.

Bartetzko, A., and K. H. Nierhaus (1988). "Mg2+/NH4+/polyamine system for polyuridine-dependent polyphenylalanine synthesis with near in vivo characteristics." Methods Enzymol **164**: 650-658.

Brenner, S. A., A. O. Stretton, and S. Kaplan (1965). "Genetic code: the 'nonsense' triplets for chain termination and their suppression." Nature **206**(988): 994-998.

Bretscher, M. S (1968). "Translocation in protein synthesis: a hybrid structure model." Nature **218**(5142): 675-677.

Brown, C. M., and W. P. Tate (1994). "Direct recognition of mRNA stop signals by Escherichia coli polypeptide chain release factor two." J Biol Chem, **269**(52): 33164-33170.

Capecchi, M. R (1967). "Polypeptide chain termination in vitro: isolation of release factor." Proc Natl Acad Sci USA **58**: 1144-1151.

Crick, F. (1970). "Central dogma of molecular biology." Nature **227**: 561-563.

Feinberg, J. S., and S. Joseph (2006). "A conserved base-pair between tRNA and 23 S rRNA in the peptidyl transferase center is important for peptide release." J Mol Biol **364**: 1010-1020.

Freistroffer, D. V., M. Kwiatkowski, R. H. Buckingham, and M. Ehrenberg (2000). "The accuracy of codon recognition by polypeptide release factors." Proc Natl Acad Sci USA **97**: 2046-2051.

Freistroffer, D. V., M. Y. Pavlov, J. MacDougall, H. Buckingham, and M. Ehrenberg (1997). "Release factor RF3 in E.coli accelerates the dissociation of release factors RF1 and RF2 from the ribosome in a GTP-dependent manner." EMBO J **16**(13): 4126-4133.

Frolova, L. Y., R. Y. Tsivkovskii, G. F. Sivolobova, N. Y. Oparina, O. I. Serpinsky, V. M. Blinov, S. I. Tatlov and L. L. Kisselev (1999). "Mutations in the highly conserved GGQ motif of class 1 polypeptide release factors abolish ability of human eRF1 to trigger peptidyl-tRNA hydrolysis." RNA **5**: 1014-1020.

Gao, H., Z. Zhou, U. Rawat, C. Huang, L. Bouakaz, C. Wang, Z. Cheng, Y. Liu, A. Zavialov, R. Gursky, S. Sanyal, M. Ehrenberg, J. Frank and H. Song (2007). "RF3 induces ribosomal conformational changes responsible for dissociation of class I release factors." Cell **129**: 929-941.

Gold, L., D. Pribnow, T. Schneider, S. Shinedling, B. S. Singer, and G. Stormo (1981). "Translational initiation in prokaryotes." Annu Rev Microbiol **35**: 365-403.

Goldstein, J. L., and C. T. Caskey (1970). "Peptide chain termination: effect of protein S on ribosomal binding of release factors." Proc Natl Acad Sci USA **67**: 537-543.

Grentzmann, G., P. J. Kelly, S. Laalami, M. Shuda, M. A. Firpo, Y. Cenatiempo and A. Kaji (1998). "Release factor RF-3 GTPase activity acts in disassembly of the ribosome termination complex." RNA **4**: 973-983.

Guthrie, C., and M. Normura (1968). "Initiation of protein synthesis: a critical test of the 30S subunit model." Nature **219**(5151): 232-235.

He, S. L., and R. Green (2010). "Visualization of codon-dependent conformational rearrangements during translation termination." Nat Struct Mol Biol **17**: 465-470.

Hetrick, B., K. Lee, and S. Joseph (2009). "Kinetics of stop codon recognition by release factor 1." Biochemistry **48**: 11178-11184.

Ito, K., M. Uno, and Y. Nakamura (2000). "A tripeptide 'anticodon' deciphers stop codons in messenger RNA." Nature **403**: 680-684.

Johnson, K. A., Ed. (1992) Transient-state kinetic analysis of enzyme reaction pathways. The Enzymes. New York, Academic.

Jorgensen, F., F. M. Adamski, W. P. Tate, and C. G. Kurkland (1993). "Release factor-dependent false stops are infrequent in Escherichia coli." J Mol Biol **230**: 41-50.

Joseph, S., and H. F. Noller (1998). "EF-G-catalyzed translocation of anticodon stem-loop analogs of transfer RNA in the ribosome." EMBO J **17**(12): 3478-3483.

Karimi, R., M. Y. Pavlov, H. Buckingham, and M. Ehrenberg (1999). "Novel roles for classical factors at the interface between translation termination and initiation." Mol Cell **3**(5): 601-609.

Klaholz, B. P., A. G. Myasnikov, and M. Van Heel (2004). "Visualization of release factor 3 on the ribosome during termination of protein synthesis." Nature **427**(6977): 862-865.

Konecki, D. S., K. C. Aune, W. Tate, and C. T. Caskey (1977). "Characterization of reticulocyte release factor." J Biol Chem **252**: 4514-4520.

Korostelev, A., H. Asahara, L. Lancaster, M. Laurberg, A. Hirschi, J. Zhu, S. Trakhanov, W. G. Scott and H. F. Noller (2008). "Crystal structure of a translation termination complex formed with release factor RF2." Proc Natl Acad Sci USA **105**: 19684-19689.

Kurland, C. G. (1960) "Molecular characterization of ribonucleic acid from Escherichia coli ribosomes I. Isolation and molecular weights." Journal of Molecular Biology **2**(2): 83-91.

Kurland, C. G. (1972). "Structure and function of the bacterial ribosome." Annu Rev Biochem **41**(10): 337-408.

Laurberg, M., H. Asahara, A. Korostelev, J. Zhu, S. Trakhanov, and H. Noller (2008). "Structural basis for translation termination on the 70S ribosome." Nature **454**: 852-857.

Lucas-Lenard, J. (1971). "Protein biosynthesis." Annu Rev Biochem **40**: 409-448.

Lucas-Lenard, J., and F. Lipmann (1966). "Separation of three microbial amino acid polymerization factors." Proc Natl Acad Sci USA **55**(6): 1562-1566.

Moazed, D., and H. F. Noller (1986). "Intermediate states in the movement of transfer RNA in the ribosome." Nature **342**(6246): 142-148.

Mortensen, K. K., F. H. Hansen, G. Grentzmann, R. H. Buckingham, and H. U. Sperling-Petersen (1995). "Osmo-expression and fast two-step purification of Escherichia coli translation termination factor RF-3." Eur J Biochem **234**: 732-736.

Myasnikov, A. G., A. Simonetti, S. Marzi, and P. Klaholz (2009). "Structure-function insights into prokaryotic and eukaryotic translation initiation." Curr Opin Struct Biol **19**(3): 300-309.

Nomura, M., and V. C. Lowry (1967). "Phage f2 RNA-directed binding of formylmethionyl-tRNA to ribosomes and the role of 30S ribosomal subunits in initiation of protein synthesis." Proc Natl Acad Sci USA **58**(3): 946-953.

Pel, H. J., J. G. Moffat, K. Ito, Y. Nakamura, and W. P. Tate (1998). "Escherichia coli release factor 3 - resolving the paradox of a typical G-protein structure and atypical function with guanine-nucleotides." RNA **4**: 47-54.

Petry, S., A. Weixlbaumer, and V. Ramakrishnan (2008). "The termination of translation." Curr Opin Struct Biol **18**(1): 70-77.

Petry, S., E. Brodersen, F. V. Murphy, C. M. Dunham, M. Selmer, M. J. Tarry, A. C. Kelley and V. Ramakrishnan (2005). "Crystal structures of the ribosome in complex with release factors RF1 and RF2 bound to a cognate stop codon." Cell **123**: 1255-1266.

Powers, T., and H. F. Noller (1991). "A functional pseudoknot in 16S ribosomal RNA." EMBO J **10**: 2203-2214.

Ramakrishnan, V. (2002). "Ribosome structure and the mechanism of translation." Cell **108**: 557-572.

Rheinberger, H. J., H. Sternbach, and H. Nierhaus (1981). "Three tRNA binding sites on Escherichia coli ribosomes." Proc Natl Acad Sci USA **78**(9): 5310-5314.

Rodnina, M. V., R. Fricke, and W. Wintermeyer (1994). "Transient conformational states of aminoacyl-tRNA during ribosome binding catalyzed by elongation factor Tu." Biochemistry **33**(40): 12267-12275.

Schmeing, T. Martin, and V. Ramakrishnan (2009). "What recent ribosome structures have revealed about the mechanism of translation." Nature **461**: 1234-1242.

Scolnick, E., R. Tompkins, T. Caskey, and M. Nirenberg (1968). "Release factors differing in specificity for terminator codons." Proc Natl Acad Sci USA **61**(2): 768-774.

Skogerson, L. K., and K. Moldave (1968). "Evidence for aminoacyl-tRNA binding, peptide bond synthesis, and translocase activities in the aminoacyl transfer reaction." Arch Biochem Biophys **125**(2): 497-505.

Stark, H., M. V. Rodnina, H. J. Wieden, M. van Heel, and W. Wintermeyer (2000). "Large-scale movement of elongation factor G and extensive conformational change of the ribosome during translocation." Cell **100**: 301-309.

Studer, S. M., J. S. Feinberg, and S. Joseph (2003). "Rapid kinetic analysis of EF-G-dependent mRNA translocation in the ribosome." J Mol Biol **327**: 369-381.

Subramanian, A. R., E. Z. Ron, and B. D. Davis (1968). "A factor required for ribosome dissociation in Escherichia coli." Proc Natl Acad Sci USA **61**(2): 761-767.

Sund, J., M. Ander, and J. Aqvist (2010). "Principles of stop-codon reading on the ribosome." Nature **465**: 947-950.

Swart, G. W., and A. Parmeggiani (1989). "tRNA and the guanosinetriphosphatase activity of elongation factor Tu." Biochemistry **28**(1): 327-332.

Traut, R. R., and R. E. Monro (1964). "The puromycin reaction and its relation to protein synthesis." J Mol Bio **10**: 63-72.

Vestergaard, B., L. B. Van, G. R. Andersen, J. Nyborg, R. H. Buckingham, and M. Kjeldgaard (2001). "Bacterial polypeptide release factor RF2 is structurally distinct from eukaryotic eRF1." Mol Cell **8**: 1375-1382.

Wiexlbaumer, A., H. Jin, C. Neubauer, R. M. Voorhees, S. Petry, A. C. Kelley and V. Ramakrishnan (2008). "Insights into translational termination from the structure of RF2 bound to the ribosome." Science **322**: 953-956.

Wimberly, B. T., D. E. Brodersen, W. M. Clemons, Jr., R. J. Morgan-Warren, A. P. Carter, C. Vonrhein, T. Hartsch and V. Ramakrishnan (2000). "Stucture of the 30S ribosomal subunit." Nature **407**(6802): 327-339.

Youngman, E. M., S. L. He, L. J. Nikstad, and R. Green (2007). "Stop codon recognition by release factors induces structural rearrangement of the ribosomal decoding center that is productive for peptide release." Mol Cell **28**: 533-543.

Yusupov, M. M., G. Z. Yusupova, A. Baucom, K. Lieberman, T. N. Earnest, J. H. Cate and H. F. Noller (2001). "Crystal structure of the ribosome at 5.5 A resolution." Science **292**(5518): 883-896.

Yusupova, G. L., L. Jenner, B. Rees, D. Moras, and M. Yusupov (2006). "Structural basis for messenger RNA movement on the ribosome." Nature **444**(7117): 391-394.

Zavialov, A. V., L. Mora, R. H. Buckingham, and M. Ehrenberg (2002). "Release of peptide promoted by the GGQ motif of class 1 release factors regulates the GTPase activity of RF3." Mol Cell **10**: 789-798.

Zavialov, A. V., R. H. Buckingham, and M. Ehrenberg (2001). "A posttermination ribosomal complex is the guanine nucleotide exchange factor for peptide release factor RF3." Cell **107**: 115-124.

Zipser, D. (1967). "UGA: a third class of suppressible polar mutants." J Mol Biol **29**: 441-445.